

# BEST\_NPZ: A ROMS BIOLOGICAL MODULE FOR THE BERING SEA

Kelly Kearney

January 26, 2019

## Contents

<b>1</b>	<b>Introduction</b>	<b>2</b>
1.1	Model History . . . . .	2
1.2	This document . . . . .	2
<b>2</b>	<b>Equation overview</b>	<b>3</b>
2.1	Summary and notation . . . . .	3
2.2	Ice formation and loss . . . . .	5
2.3	Source-minus-sink processes . . . . .	6
2.3.1	Light attenuation in water . . . . .	6
2.3.2	Gross primary production . . . . .	7
2.3.3	Grazing and predation . . . . .	10
2.3.4	Egestion and excretion . . . . .	13
2.3.5	Respiration . . . . .	13
2.3.6	Mortality and senescence . . . . .	15
2.3.7	Remineralization and nitrification . . . . .	16
2.3.8	Ice interface convective exchange . . . . .	16
2.3.9	Total rate of change . . . . .	17
2.4	Vertical movement and exchanges . . . . .	19
2.4.1	Sinking of phytoplankton and detritus . . . . .	19
2.4.2	Copepod diapause . . . . .	19
2.4.3	Euphausiid diel vertical migration . . . . .	20
2.5	Analytical relaxation of state variables . . . . .	20
<b>3</b>	<b>Compilation flags</b>	<b>22</b>
<b>4</b>	<b>Output variables</b>	<b>25</b>
<b>5</b>	<b>Internal dynamics of the BEST-NPZ model in the Bering Sea</b>	<b>31</b>
<b>6</b>	<b>References</b>	<b>37</b>

# 1 Introduction

The Bering Sea supports a diverse ecosystem of fish, birds, and mammals, as well as one of the largest fisheries in the world, accounting for approximately 40% of the US commercial fisheries catch. The high production in this region is possible due to many physical characteristics unique to the region, including a broad shelf, strong tides, and the presence of seasonal sea ice. These characteristics also complicate the modeling of this environment, since the mechanisms controlling primary and secondary production span the pelagic, benthic, and sympagic (ice) habitats.

The Bering Ecosystem Study Nutrient Phytoplankton Zooplankton model, i.e. BEST\_NPZ, model, was developed in an attempt to capture the relevant processes controlling ecosystem production in the Bering Sea. The model is designed to be coupled and run within the Regional Ocean Modeling System (ROMS) framework (Shchepetkin & McWilliams, 2005; Haidvogel et al., 2008).

## 1.1 Model History

The BEST\_NPZ model has undergone several phases of development in the hands of several different researchers. The code for the pelagic system originated from Sarah Hinckley's Gulf of Alaska NPZ model (Hinckley et al., 2009), i.e. GOANPZ. Model parameters and equations were tailored to the Bering Sea ecosystem during the Bering Ecosystem Study<sup>1</sup> and Bering Sea Integrated Ecosystem Research Project<sup>2</sup>, and the benthic and sympagic modules were added to the code during this phase. Development then diverged, with one set of collaborators focusing on further development of the primary and secondary production portions of the model (Gibson & Spitz, 2011), primarily in a one-dimensional idealized environment representing the M2 mooring location (56.87°, -164.06°), and a second group using the existing model as a base for a size- and age-structured forage fish model, known as FEAST (Aydin, unpublished) within the three-dimensional Bering 10K ROMS domain (Hermann et al., 2013). In 2016, we (i.e. your current narrator, in collaboration with the aforementioned groups) merged those two lines of development, extending the improvements to the biogeochemical formulations and parameters from the one-dimensional model to be fully compatible with the three-dimensional Bering 10K grid. Following that, we proceeded to overhaul the internal code base for better maintainability, as well as to update model equations and parameters based on more recent validation.

<sup>1</sup> BEST: <https://www.nprb.org/bering-sea-project/about-the-project/>

<sup>2</sup> BSIERP: <http://bsierp.nprb.org>

## 1.2 This document

This documentation reflects the most up-to-date version of the BEST\_NPZ model as maintained by the author. This particular version of the code is available for viewing and download on GitHub<sup>3</sup>. Development and validation of the model continues, with the intent to keep this accompanying documentation current with the code.

In [section 2](#), we provide a mathematical description of the BEST\_NPZ model. We also document the biological input parameters used in these equations; the parameters are passed to ROMS via the biological input parameter file when running this module.

ROMS uses a C preprocessor to selectively compile code variants; the compilation flags associated with the BEST\_NPZ biological module can be found in [section 3](#). This section is primarily intended for current and future developers of the code.

Finally, [section 4](#) provides a complete list of output variables, including both prognostic state variables and diagnostic variables, that can be added to the ROMS output files when running the BEST\_NPZ model. This is intended primarily for researchers who will be working directly with this model's output or running new simulations themselves.

We make ample use of margin notes and figures throughout this paper. They are used to note where model equations and parameters may be (more) uncertain, to clarify and compare functions, to explain the origin of certain numbers, etc. The tone of these margin notes is intentionally informal; the intent is to simply keep all aspects of this model's internal workings (and the decisions that led there) as transparent as possible, and this requires the occasional informal musing.

<sup>3</sup> GitHub repository: <https://github.com/kakearney/roms-bering-sea> (currently a private repository; contact author for access)

## 2 Equation overview

### 2.1 Summary and notation

This section provides a mathematical overview of processes through which biological state variables exchange material with each other in the BEST\_NPZ model.

The BEST\_NPZ model assumes a model geometry that includes  $N$  water column layers, a single benthic layer of unspecified depth, and a skeletal ice layer with a constant thickness  $h_{sice}$ . Within this geometry, it tracks the concentration of 19 biological state variables:

**Table 1** – Biological state variables in the BEST\_NPZ model.

Index	Variable	Description	Units
1	NO3	nitrate	mmolN/m <sup>3</sup>
2	NH4	ammonium	mmolN/m <sup>3</sup>
3	PhS	small phytoplankton (cells less than 10 $\mu$ m diameter)	mgC/m <sup>3</sup>
4	PhL	large phytoplankton (bloom forming diatoms)	mgC/m <sup>3</sup>
5	MZL	microzooplankton	mgC/m <sup>3</sup>
6	Cop	small-bodied copepods (e.g. <i>Pseudocalanus</i> spp.)	mgC/m <sup>3</sup>
7	NCaS	on-shelf large-bodied copepods (primarily <i>Calanus marshallae</i> )	mgC/m <sup>3</sup>
8	EupS	on-shelf euphausiids (primarily <i>Thysanoessa raschii</i> )	mgC/m <sup>3</sup>
9	NCaO	off-shelf large-bodied copepods (primarily <i>Neocalanus</i> spp.)	mgC/m <sup>3</sup>
10	EupO	off-shelf euphausiids (primarily <i>Thysanoessa inermis</i> )	mgC/m <sup>3</sup>
11	Det	slow-sinking detritus	mgC/m <sup>3</sup>
12	DetF	fast-sinking detrituse	mgC/m <sup>3</sup>
13	Jel	jellyfish ( <i>Chrysaora melanaster</i> )	mgC/m <sup>3</sup>
14	Fe	iron	$\mu$ molFe/m <sup>3</sup>
15	Ben	benthic infauna (bivalves, amphipods, polychaetes, etc.)	mgC/m <sup>2</sup>
16	BenDet	benthic detritus	mgC/m <sup>2</sup>
17	IcePhL	ice algae	mgC/m <sup>3</sup>
18	IceNO3	ice nitrate	mmolN/m <sup>3</sup>
19	IceNH4	ice ammonium	mmolN/m <sup>3</sup>

Exchange of material between these state variables, and across vertical layers within a single state variable, results from a variety of processes. In the code, and in this description, these processes are divided into three types.

The first type of process, described in [section 2.2](#), includes redistribution of state variables due to movement of the water or ice in which they reside. The majority of these calculations (e.g. advection and diffusion of water and ice) take place outside the biological module. The one exception is the exchange of NO3 and IceNO3, NH4 and IceNH4, and PhL and IcePhL due to the formation or loss of ice in a grid cell.

The second process type we term source-minus-sink processes ([section 2.3](#)); these processes take place within a single depth layer<sup>4</sup> and involve transfer of biomass from one state variable to another. For notation, each source-minus-sink flux process is represented in this document as a function of the source and sink state variables, respectively. For example,  $Abc(X, Y)$  is the flux rate of material from group X to group Y via the  $Abc$  process.

The final category ([section 2.4](#)) is vertical movement, where the concentration of state variables is redistributed within the water column due to sinking or rising movement of the state variables within the water (note that this is separate from vertical advection of tracers due to movement of the water itself.)

The three types of processes are calculated sequentially in the code, such that changes due to ice loss and formation are calculated first, followed by the total rate of change due to source-minus-sink processes, and finally redistribution due to vertical movement<sup>5</sup>.

Several of the equations in this section rely on state or diagnostic variables that come from

<sup>4</sup> with a few exceptions for exchange between the water column and the ice and benthic layers

<sup>5</sup> When the BEST\_NPZ module is coupled to the FEAST upper trophic level model, the FEAST-specific calculations are added as a fourth step, after all biological iterations of the BEST\_NPZ model are completed (i.e. the BioIter subdivisions apply to the three abovementioned process steps, but not to FEAST).

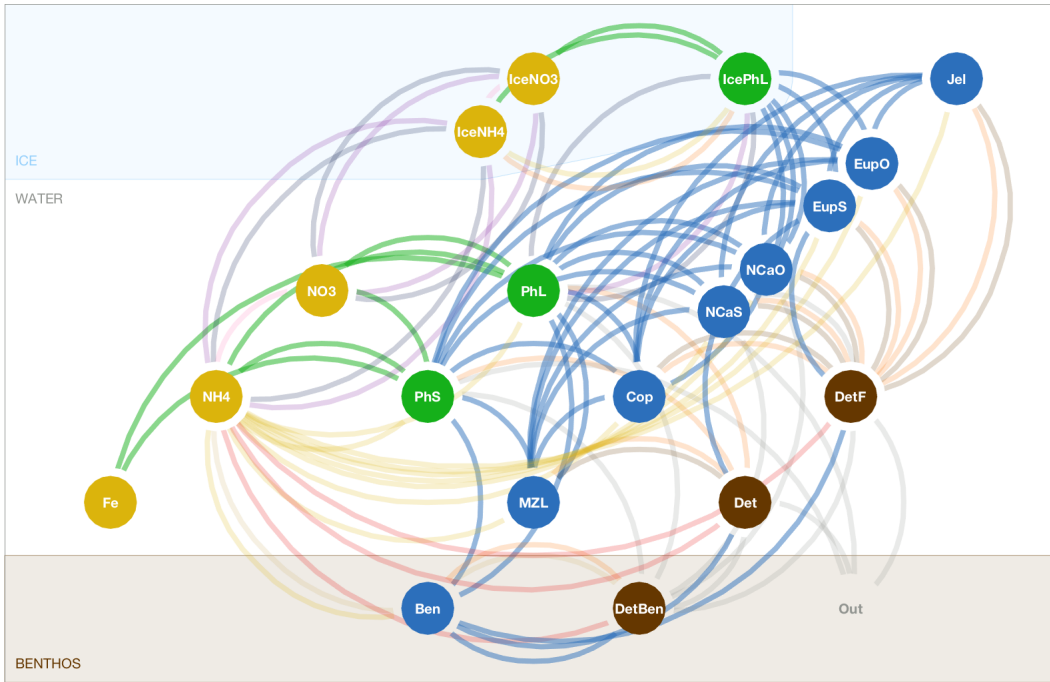


**Figure 1** – Schematic of the BEST\_NPZ model. Edges (lines) represent fluxes between state variables (gold = nutrient, green = producer, blue = consumer, brown = detritus), and curve clockwise from source node to sink node. Edge colors indicate process type: green = primary production, blue = grazing and predation, brown = egestion, gold = respiration, red = remineralization, pink = nitrification, orange = non-predatory mortality, tan = excretion, purple = convective exchange, gray = sinking to seafloor, navy = freezing/melting of ice

the physical model or from the ROMS grid geometry. See [Table 2](#) for a description of these variables and their notation in this document. Additional parameters derived from biological input parameters are listed in [Table 3](#).

**Table 2** – Notation and description for variables deriving from the physical model.

Variable	Name	Units	Details
$z$	depth	m	relative to mean sea level (positive above mean sea level, negative below)
$\zeta$	free surface height	m	relative to mean sea level
$h$	bathymetry	m	depth of the ocean floor in a given grid cell, measured from mean sea level and expressed as a positive number
$h_k$	thickness of depth layer $k$	m	varies as a function of $h$ and $\zeta$ , $k = 1$ corresponds to bottom layer and $k = N$ to the top layer
$h_{ice}$	thickness of sea ice	m	
$a_{ice}$	fraction of grid cell covered by sea ice	--	
$T$	temperature	°C	
$\epsilon$	machine epsilon	--	small value used to avoid 0 problems
$c_I$	light conversion factor	$E m^{-2} d^{-1} W^{-1} m^2$	<a href="#">Thimijan &amp; Heins (1983)</a> provide the conversion factor of $4.57 \mu E s^{-1} m^{-2}$ per $1 W m^{-2}$ (i.e. $0.394848 E m^{-2} d^{-1} W^{-1} m^2$ ) for the 400-700 nm band assuming a light source of "sun and sky, daylight".

$I_0$	surface irradiance	$\text{E m}^{-2} \text{d}^{-1}$	converted from surface heat flux to photon flux assuming seawater density = $1025 \text{ kg m}^{-3}$ , heat capacity = $3985 \text{ J kg}^{-1} \text{ }^\circ\text{C}^{-1}$ , and absorption wavelengths appropriate to chlorophyll (see $c_I$ , above). Note that this represents below-ice irradiance when ice is present.
-------	--------------------	---------------------------------	--

**Table 3** – Notation and description for input parameters applicable to all biomass rate of change processes.

Variable	Description	Units	Relevant input parameter(s)		
			Group	Parameter	Value
$h_{sice}$	thickness of skeletal ice layer	m		aidx	0.02
$\xi$	N:C ratio	$\text{mmol}_\text{N} \text{ mg}_\text{C}^{-1}$		xi	0.0126
$FeC$	Fe:C ratio	$\mu\text{mol}_\text{Fe} \text{ mg}_\text{C}^{-1}$		FeC	0.000 166 7

To express the concentration of a biological state variable  $X$ , we use the notation  $[X]$ , with units corresponding to those in Table 1. All intermediate fluxes are expressed in terms of  $\text{mgC}$  for simplicity. Conversions between units assume constant stoichiometry for all living and detrital groups.

Because many of the variable names used in these equations involve multi-letter and mixed-case notations, we've chosen to use dot notation for all instances of multiplication in this document. Please note that this indicates simple element-by-element multiplication in the BEST\_NPZ code, not a dot product.

## 2.2 Ice formation and loss

Although the primary ROMS sea ice model tracks ice presence in terms of fraction grid cell coverage, the BEST\_NPZ biological module uses a simpler scheme where ice presence is treated as a binary condition. When the ice thickness ( $h_{ice}$ ) in a grid cell is greater than the prescribed thickness of the skeletal ice layer ( $h_{sice}$ ) and the grid cell has at least 50% ice cover (as indicated by the  $a_{ice}$  variable), we assume the entirety of that grid cell now supports the ice-related biological processes in a thin layer of skeletal ice covering the entire grid cell and located just above the free surface of that grid cell.

If sea ice appears in a grid cell between the previous time step and the current time step, the large phytoplankton, nitrate, and ammonium in the top layer are redistributed evenly between the top water column layer and the skeletal ice layer.<sup>6</sup>

$$[\text{IcePhL}]_{ice} = \frac{[\text{PhL}]_{k=N} \cdot h_{k=N}}{h_{sice} + h_{k=N}} \quad (1)$$

$$[\text{PhL}]_{k=N} = \frac{[\text{PhL}]_{k=N} \cdot h_{k=N}}{h_{sice} + h_{k=N}} \quad (2)$$

$$[\text{IceNO3}]_{ice} = \frac{[\text{NO3}]_{k=N} \cdot h_{k=N}}{h_{sice} + h_{k=N}} \quad (3)$$

$$[\text{NO3}]_{k=N} = \frac{[\text{NO3}]_{k=N} \cdot h_{k=N}}{h_{sice} + h_{k=N}} \quad (4)$$

$$[\text{IceNH4}]_{ice} = \frac{[\text{NH4}]_{k=N} \cdot h_{k=N}}{h_{sice} + h_{k=N}} \quad (5)$$

$$[\text{NH4}]_{k=N} = \frac{[\text{NH4}]_{k=N} \cdot h_{k=N}}{h_{sice} + h_{k=N}} \quad (6)$$

Likewise, when ice disappears between the previous step and the current one, all material in the skeletal ice layer is moved to the top layer of the water.

<sup>6</sup> This calculation assumes that nutrients freeze in place when ice is formed, rather than being extruded. Not sure if that's how it works in the real world, but this assumption has negligible impact on the model dynamics due to the presence of convective exchange between the ice and the surface layer.

$$[\text{PhL}]_{k=N} = \frac{[\text{PhL}]_{k=N} \cdot h_{k=N} + [\text{IcePhL}_{ice}] \cdot h_{sice}}{h_{k=N}} \quad (7)$$

$$[\text{NO3}]_{k=N} = \frac{[\text{NO3}]_{k=N} \cdot h_{k=N} + [\text{IceNO3}_{ice}] \cdot h_{sice}}{h_{k=N}} \quad (8)$$

$$[\text{NH4}]_{k=N} = \frac{[\text{NH4}]_{k=N} \cdot h_{k=N} + [\text{IceNH4}_{ice}] \cdot h_{sice}}{h_{k=N}} \quad (9)$$

$$[\text{IcePhL}]_{ice} = 0 \quad (10)$$

$$[\text{IceNO3}]_{ice} = 0 \quad (11)$$

$$[\text{IceNH4}]_{ice} = 0 \quad (12)$$

## 2.3 Source-minus-sink processes

Unless otherwise specified, all processes detailed in this section are specific to a single layer. We have used the subscript  $k$  when defining each layer-specific flux rate;  $k$  can be either the index of a water column layer, or  $sice$  to indicate the skeletal ice layer. This notation distinguishes between rates that are specific to a single layer, and that use volumetric units ( $\text{mgC}/\text{m}^3/\text{d}$ ) versus those that exchange material between layers and that are expressed in total flux across a boundary ( $\text{mgC}/\text{m}^2/\text{d}$ ). To avoid clutter, we have chosen not to apply these subscripts to any remaining layer-dependent variables (such as state variable concentrations), but these are to be assumed for all pelagic and ice layer components.

### 2.3.1 Light attenuation in water

The model assumes that radiation is attenuated with depth as follows:

$$I_z = f_{PAR} \cdot I_0 \cdot \exp(-K_{PAR} \cdot (\zeta - z)) \quad (13)$$

where  $f_{PAR}$  is the fraction of surface light that is photosynthetically available,  $I_0$  is the surface irradiance, and  $K_{PAR}$  is the light attenuation coefficient for photosynthetically active radiation (i.e. 400-700 nm). Incoming radiation is supplied by the physical model and converted to photon flux. Currently, the value of  $f_{PAR}$  is set based on an approximate fit between our hindcast shortwave radiation and satellite-measured photosynthetically active radiation across the Bering Sea domain (Figure 2).

The attenuation coefficient is itself the sum of attenuation from clear water, chlorophyll, and other organic material:

$$K_{PAR} = K_w + K_A \cdot \left( \frac{[\text{PhL}]}{ccr_L} + \frac{[\text{PhS}]}{ccr_S} \right)^{K_B} + K_C + K_{D1} \cdot h^{K_{D2}} \quad (14)$$

The first three terms in Equation 14 derive from Morel (1988)'s analysis of light attenuation in Case I waters. The final term (i.e. the  $K_D$  portion) adds additional attenuation based on the depth of the water column; this approximates the assumption that sediment and organic material is higher near the coastline than in open water. The power law formula was chosen based on a fit to satellite-derived inherent optical properties across the Bering Sea domain (Figure 3).

The  $K_{PAR}$  parameter is also used to calculate shortwave radiation decay in the physical model. In this case, we use a modified version of the Paulson & Simpson (1977) equation for attenuation:

$$f_{swdk} = (1 - a_{frac}) \cdot \exp(-K_{PAR} \cdot (\zeta - z)) + a_{frac} \cdot \exp\left(\frac{-(\zeta - z)}{a_{\mu 1}}\right) \quad (15)$$

The values of  $a_{frac}$  and  $a_{\mu 1}$  correspond to  $R$  and  $\zeta_2$  in Paulson & Simpson (1977), with our  $K_{PAR}$  replacing Paulson & Simpson (1977)'s  $\zeta_1$ ; we use the parameter values for Case I waters.

**Table 4** – Notation and description for input parameters related to light attenuation.

**Figure 2** – Deriving  $f_{PAR}$ : Our estimate is based on a comparison of shortwave radiation in our forcing files and satellite-derived PAR.

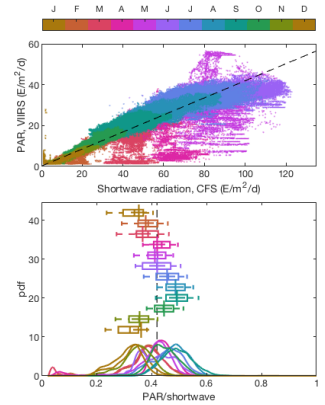
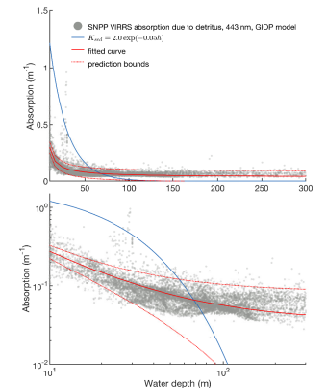


**Figure 3** – Attenuation due to sediment was estimated by fitting the satellite-derived estimations of absorption due to gelbstoff and detrital material (entire mission composite from VIIRS, 2012-2018). Panels show same data, in linear and logarithmic space.



Variable	Description	Units	Relevant input parameter(s)		
			Group	Parameter	Value
$f_{PAR}$	PAR fraction (fraction of shortwave that's in the 400-700 nm band)	--		PARfrac	0.42
$ccr_S$	C:chl ratio	mgC mg <sup>-1</sup> <sub>chl<sub>a</sub></sub>	PhS	ccr	65
$ccr_L$	C:chl ratio	mgC mg <sup>-1</sup> <sub>chl<sub>a</sub></sub>	PhL	ccrPhL	25
$a_{frac}$	a unitless coefficient that determines switch between deep water and shallow water attenuation	--		a_frac hardcoded parameter	0.58
$a_{\mu 1}$	attenuation length scale for deeper water	m <sup>-1</sup>		a_mu1 hardcoded parameter	0.35
$K_W$	attenuation coefficient for clear water	m <sup>-1</sup>		k_ext	0.034
$K_A$	factor, attenuation coefficient for chlorophyll	m <sup>-1</sup>		k_chlA	0.0518
$K_B$	exponent, attenuation coefficient for chlorophyll	--		k_chlB	0.428
$K_C$	attenuation coefficient for other material (CDOM, sediment, etc.)	m <sup>-1</sup>		k_chlC	0
$K_{D1}$	factor, depth-based attenuation coefficient	m <sup>-1</sup>		k_sed1	2.833
$K_{D2}$	exponent, depth-based attenuation coefficient	--		k_sed2	-1.079

### 2.3.2 Gross primary production

Primary production for both small and large phytoplankton is governed by the same set of equations. The maximum photosynthetic growth rate per unit chlorophyll (mgC/mgChl<sub>a</sub>/d) is a function of temperature, and defined in terms of each group's doubling rate  $D_i$  and doubling rate exponent  $D_p$  (Frost, 1987). The maximum uptake rate is calculated in both carbon-specific and chlorophyll-specific units:

$$P_{max} = \left( 2^{(D_i \cdot 10^{(D_p \cdot T)})} - 1 \right) \quad (16)$$

$$P_{max}^* = P_{max} \cdot ccr \quad (17)$$

This rate is moderated by light and nutrient limitation. Light limitation uses a hyperbolic tangent function, after Jassby & Platt (1976),

$$Lim_I = \tanh \left( \frac{\alpha \cdot I_z}{P_{max}^*} \right) \quad (18)$$

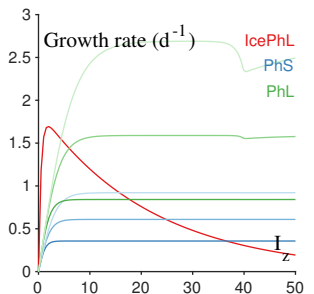
For earlier versions of the model,  $\alpha$  was set to a constant value for each phytoplankton group, following Strom et al. (2010). However, more recent measurements (Strom et al., 2016) suggest that phytoplankton can adapt to varying light levels, increasing their photosynthetic efficiency under low light conditions. To mimic this behavior (without the additional complexity that comes with varying Chl:C ratios),  $\alpha$  is now defined as a function of light<sup>7</sup>:

$$\alpha = \begin{cases} \alpha_{lo} & I_z < I_{lo} \\ \alpha_{lo} - \left( \frac{\alpha_{lo} - \alpha_{hi}}{I_{hi} - I_{lo}} \cdot I_z \right) & I_{lo} \leq I_z \leq I_{hi} \\ \alpha_{hi} & I_z > I_{hi} \end{cases} \quad (19)$$

Nutrient limitation is based on the availability of nitrate, iron, and ammonium. Nitrate limitation uses Michaelis-Menten uptake with ammonium inhibition (Wroblewski, 1977):

$$Lim_{NO3} = \frac{[NO3]}{k_1 + [NO3]} \cdot \exp(-\psi \cdot [NH4]) \quad (20)$$

Figure 4 – Nutrient-replete growth rate at -2°C (darkest), 5°C, and 10°C (lightest).



<sup>7</sup> I'm not convinced this is achieving its intended purpose; the shifts in production rate are... odd. Most recent run has returned to the constant alpha equation until I work out a better option.

Ammonium limitation is also formulated with Michaelis-Menten:

$$Lim_{NH4} = \frac{[NH4]}{k_2 + [NH4]} \quad (21)$$

Macronutrient uptake is partitioned between ammonium and nitrate using an f-ratio ( $f_{new}$ ) paired with total nitrogen limitation:

$$f_{new} = \frac{Lim_{NO3}}{Lim_{NO3} + Lim_{NH4}} \quad (22)$$

$$Lim_N = \min(Lim_{NO3} + Lim_{NH4}, 1.0) \quad (23)$$

Iron limitation can be included via the IRON\_LIMIT compilation flag:

$$Lim_{Fe} = \min\left(1.0, \epsilon + \frac{[Fe]}{k_{Fe} + [Fe]} \cdot \frac{k_{Fe} + Fe_{Crit}}{Fe_{Crit}}\right) \quad (24)$$

Without the IRON\_LIMIT flag,  $Lim_{Fe} = 1$ . The iron limitation model is a simple one, following [Hinckley et al. \(2009\)](#); it is assumed to limit nitrate uptake due to iron's role in the reduction of nitrate during photosynthesis.<sup>8</sup> Light and nutrient limitation are applied following a minimum threshold colimiting equation ([Denman & Pena, 1999](#)):

$$Gpp(NO3, X)_k = P_{max} \cdot [X] \cdot \min(Lim_N \cdot Lim_{Fe}, Lim_I) \cdot f_{new} \quad (25)$$

$$Gpp(NH4, X)_k = P_{max} \cdot [X] \cdot \min(Lim_N \cdot Lim_{Fe}, Lim_I) \cdot (1 - f_{new}) \quad (26)$$

Primary production also occurs in the ice layer when ice is present. In the ice layer, production is a function of light, nutrient limitation, brine salinity, and temperature, following [Jin et al. \(2006\)](#). Light limitation uses the following photosynthesis-irradiance curve; unlike the pelagic production, this one includes strong photoinhibition at higher light levels:

$$Lim_{Ice} = \left(1 - \exp\left(-\alpha_{Ib} \cdot \frac{I_0 \cdot f_{PAR}}{c_I}\right)\right) \cdot \exp\left(-\beta_I \cdot \frac{I_0 \cdot f_{PAR}}{c_I}\right) \quad (27)$$

where  $\frac{I_0 \cdot f_{PAR}}{c_I}$  is the photosynthetically active radiation converted to  $W m^{-2}$ .

As in the water column, nitrate limitation uses Michaelis-Menten uptake dynamics with ammonium inhibition (with  $f_r$  denoting the f-ratio between new (nitrate) and regenerated (ammonium) production):

$$Lim_{Nice} = \frac{[IceNO3]}{k_1 + [IceNO3]} \cdot \exp(-\psi \cdot [IceNH4]) + \frac{[IceNH4]}{k_2 + [IceNH4]} \quad (28)$$

$$f_r = \frac{\frac{[IceNO3]}{k_1 + [IceNO3]} \cdot \exp(-\psi \cdot [IceNH4])}{Lim_{Nice}} \quad (29)$$

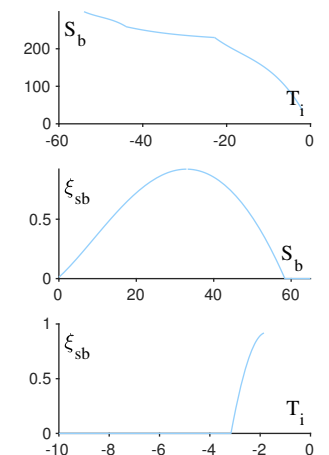
Brine salinity ( $S_b$ ) is not tracked explicitly by the ice model, so instead it is estimated based on a piecewise polynomial fit to ice temperature ( $T_i$ , tracked by the the ice model), following [Arrigo et al. \(1993\)](#):

$$S_b = c_0 + c_1 \cdot T_i + c_2 \cdot T_i^2 + c_3 \cdot T_i^3 \quad (30)$$

	$c_0$	$c_1$	$c_2$	$c_3$
$T_i \geq -22.9$	-3.9921	-22.7	-1.0015	-0.019956
$-44.0 < T_i < -22.9$	206.24	-1.8907	-0.060868	-0.0010247
$T_i \leq -44.0$	-4442.1	-277.86	-5.501	-0.03669

<sup>8</sup> As currently coded, the iron limitation affects both NO3 and NH4 uptake, similar to [Coyle et al. \(2012\)](#). But more recent versions of GOANPZ seem to follow the reduction-of-nitrate idea and only apply it to nitrate uptake. May want to revisit this in our model... but will need to make sure f-ratio is modified appropriately.

**Figure 5** – Ice-related polynomials



The effect of salinity on ice algae growth rate is also a polynomial fit (Arrigo & Sullivan, 1992):

$$\begin{aligned} \xi_{sb} = & 1.1 \times 10^{-2} + 3.012 \times 10^{-2} \cdot S_b \\ & + 1.0342 \times 10^{-3} \cdot S_b^2 \\ & - 4.6033 \times 10^{-5} \cdot S_b^3 \\ & + 4.926 \times 10^{-7} \cdot S_b^4 \\ & - 1.659 \times 10^{-9} \cdot S_b^5 \end{aligned} \quad (31)$$

When running in climatological ice mode (CLIM\_ICE\_1D), where no explicit ice temperature is modeled,  $\xi_{sb} = 1.0$ .

The final primary production calculation is then:

$$Gpp(\text{IceNO}_3, \text{IcePhL})_{ice} = \mu_0 \cdot \exp(0.0633 \cdot T_{k=N}) \cdot \xi_{sb} \cdot \min(Lim_{Ice}, Lim_{N_{ice}}) \cdot [\text{IcePhL}] \cdot f_r \quad (32)$$

$$Gpp(\text{IceNH}_4, \text{IcePhL})_{ice} = \mu_0 \cdot \exp(0.0633 \cdot T_{k=N}) \cdot \xi_{sb} \cdot \min(Lim_{Ice}, Lim_{N_{ice}}) \cdot [\text{IcePhL}] \cdot (1 - f_r) \quad (33)$$

In this case,  $T_{k=N}$  is the temperature of the top water layer, used to approximate the temperature of the ice itself<sup>9</sup>.

<sup>9</sup> Should we add a switch in the code so it uses actual ice temperature when it's available, and only falls back on surface water temperature when in climatological ice mode? Or is surface temperature more appropriate for the temperature of the base of the ice?

**Table 5** – Notation and description for input parameters related to gross primary production.

Variable	Description	Units	Relevant input parameter(s)		
			Group	Parameter	Value
$\alpha_{lo}$	photosynthetic efficiency, low light	$\text{mg}_C \text{mg}_{\text{chla}}^{-1} \text{E}^{-1} \text{m}^2$	PhS	hardcoded	18
			PhL	hardcoded	10
$\alpha_{hi}$	photosynthetic efficiency, high light	$\text{mg}_C \text{mg}_{\text{chla}}^{-1} \text{E}^{-1} \text{m}^2$	PhS	hardcoded	5.6
			PhL	hardcoded	2.2
$I_{lo}$	low light threshold for PI curve slope transition	$\text{E m}^{-2} \text{d}^{-1}$	PhS	hardcoded	30
			PhL	hardcoded	30
$I_{hi}$	high-light threshold for PI curve slope transition	$\text{E m}^{-2} \text{d}^{-1}$	PhS	hardcoded	40
			PhL	hardcoded	40
$K_1$	half-saturation constant for nitrate uptake	$\text{mmol}_N \text{m}^{-3}$	PhS	k1PhS	1
			PhL	k1PhL	2
			IcePhL	ksnut1	1
$K_2$	half-saturation constant for ammonium uptake	$\text{mmol}_N \text{m}^{-3}$	PhS	k2PhS	0.5
			PhL	k2PhL	2
			IcePhL	ksnut2	4
$\psi$	ammonium inhibition constant	$\text{m}^3 \text{mmol}_N^{-1}$	PhS	psiS	1.5
			PhL	psiL	1.5
			IcePhL	inhib	1.46
$D_i$	doubling rate parameter	$\text{d}^{-1}$	PhS	DiS	0.5
			PhL	DiL	1
$D_p$	doubling rate parameter	$^{\circ}\text{C}^{-1}$	PhS	DpS	0.0275
			PhL	DpL	0.0275
$k_{Fe}$	half-saturation constant for iron uptake	$\mu\text{mol}_{\text{Fe}} \text{m}^{-3}$	PhS	kfePhS	0.3
			PhL	kfePhL	1
$Fe_{Crit}$	iron concentration below which growth is limited	$\mu\text{mol}_{\text{Fe}} \text{m}^{-3}$	PhS	FeCritPS	2
			PhL	FeCritPL	2
$\alpha_{Ib}$	photosynthetic efficiency/maximal photosynthetic rate	$\text{W m}^{-2}$	IcePhL	alphaIb	0.08

$\beta_I$	light inhibition/maximal photosynthetic rate	$\text{W m}^{-2}$	IcePhL	betaI	0.018
$\mu_0$	maximum growth rate at 0 deg C	$\text{d}^{-1}$	IcePhL	mu0	2.4

### 2.3.3 Grazing and predation

Pelagic grazing and predation fluxes are a function of a grazer or predator's maximum ingestion rate ( $e_Y$ ), its total prey availability, prey-specific feeding preferences ( $fp_{XY}$ ) (Figure 6), and the water temperature, using the multiple resource Holling Type 3 functional response of Ryabchenko et al. (1997):

$$Gra(X, Y)_k = Q_Y^{\left(\frac{T-Q_{TY}}{10}\right)} \cdot e_Y \cdot [Y] \cdot \frac{fp_{XY} \cdot [X]^2}{f_Y + \sum_Z (fp_{ZY} \cdot [Z]^2)} \quad (34)$$

where Y refers to the predator group, X is a specific prey group, and Z refers to the set of all prey groups of that predator. Note that some of the pelagic groups can graze on ice algae; when preyed upon, the ice algae concentration is adjusted as though it were located in the surface layer of the water:

$$[IcePhL]_k = \begin{cases} [IcePhL]_{ice} \cdot \frac{h_{sice}}{h_k}, & k = N \\ 0, & \text{otherwise} \end{cases} \quad (35)$$

The maximum ingestion rates,  $e_Y$ , are constant for all groups except large-bodied copepods (NCaS and NCaO). These groups can be parameterized to perform seasonal diapause, and during periods of downward migration, their ingestion rates are dropped to  $e_Y = 0 \text{ d}^{-1}$ . See section 2.4 for a description of the diapause time-of-year calculation.

When the DEPTHLIMITER<sup>10</sup> compilation option is defined, the two euphausiid groups include an additional ingestion rate modifier term that effectively turns off grazing by EupS in water deeper than 200m depth and for EupO in water shallower than 200m. This is based on anecdotal observations that the two groups are typically found in different depth environments.

Benthic processes in BEST\_NPZ are based on a greatly-simplified version of the European Regional Seas Ecosystem model (ERSEM) (Ebenhöh et al., 1995). Benthic infauna graze on pelagic detritus and phytoplankton located within a certain distance of the bottom (currently hard-coded to  $dw = 1.0\text{m}$ ). The feeding fluxes are defined as follows<sup>11</sup>:

$$[X]_{ben} = \int_{-h}^{-h+dw} [X] dz \quad (36)$$

$$F_X = \frac{(fp_{XB} \cdot [X]_{ben})^2}{fp_{XB} \cdot [X]_{ben} + L_P} \quad (37)$$

$$Gra(X, Ben) = Q_B^{\left(\frac{T-Q_{TB}}{10}\right)} \cdot e_{Ben} \cdot [Ben] \cdot \frac{F_X}{\sum_Z F_Z + f_{PB}} \quad (38)$$

As in the pelagic grazing equation, X refers to a single pelagic prey group (PhS, PhL, Det, or DetF), and Z refers to the full set of these four groups. A weight factor,  $w_{k,X}$  is calculated to distribute these losses proportionately across the water column (see section 2.3.9):

$$w_{k,X} = \frac{\int_{z_{lo,k}}^{\min(z_{hi,k}, -h+dw)} [X] dz}{[X]_{ben}} \quad (39)$$

where  $z_{lo,k}$  and  $z_{hi,k}$  are the lower and upper depth limits of layer  $k$ .

Benthic infauna also graze on benthic detritus, following the same equation but with different parameters for prey threshold and half-saturation values:

Figure 6 – Feeding preferences.

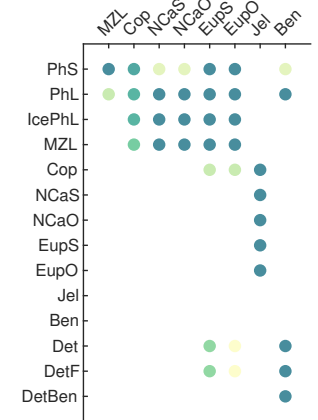
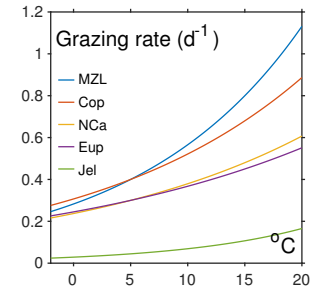


Figure 7 – Maximum ingestion rates.



<sup>10</sup> I don't particularly like this death-ray approach to force two nearly identical functional groups to stay where they "belong". For both the euphausiid and copepod groups, I would like to further investigate whether the two species play different functional roles in the ecosystem. If not, the separation of functional groups is an unnecessary bit of added complexity, and the groups should be combined. If so, what are the underlying mechanisms that lead to the observed segregation of species? (prey preference? energy storage? reproduction strategies?) For now, we usually keep the depth-limiter flag off, and the onshore and offshore groups are both found throughout the domain.

$$F_X = \frac{(fp_{XB} \cdot [X])^2}{fp_{XB} \cdot [X] + L_D} \quad (40)$$

$$Gra(X, Ben) = Q_B^{\left(\frac{T-Q_{TB}}{10}\right)} \cdot e_{Ben} \cdot [Ben] \cdot \frac{F_X}{F_X + f_{DB}} \quad (41)$$

Here, X refers to a single prey group, BenDet.

Note that the water column grazing fluxes are in units of mgC/m<sup>3</sup>/d while the benthic feeding fluxes are in mgC/m<sup>2</sup>/d.

<sup>11</sup> Pelagic and benthic feeding equations are similar, but the use of the feeding preference term is a little different in the two formulas. I assume this is simply due to the different source references for the two components, since the benthos submodel was added late in the development. We might consider moving code toward a unified formula, to avoid any spurious results from the equation differences.

**Table 6** – Notation and description for input parameters related to grazing and predation.

Variable	Description	Units	Relevant input parameter(s)		
			Group	Parameter	Value
$fp_{XY}$	grazing preference of predator Y on prey X	--	PhS → MZL	fpPhSMZL	1
			PhL → MZL	fpPhLMZL	0.2
			PhS → Cop	fpPhSCop	0.8
			PhL → Cop	fpPhLCop	0.7
			MZL → Cop	fpMZLCop	0.5
			IcePhL → Cop	fpPhLCop	0.7
			PhS → NCaS	fpPhSNCa	0.1
			PhL → NCaS	fpPhLNCa	1
			MZL → NCaS	fpMZLNCa	1
			IcePhL → NCaS	fpPhLNCa	1
			PhS → NCaO	fpPhSNCa	0.1
			PhL → NCaO	fpPhLNCa	1
			MZL → NCaO	fpMZLNCa	1
			IcePhL → NCaO	fpPhLNCa	1
			PhS → EupS	fpPhSEup	1
			PhL → EupS	fpPhLEup	1
			MZL → EupS	fpMZLEup	1
			Cop → EupS	fpCopEup	0.2
			Det → EupS	fpDetEup	0.4
			DetF → EupS	fpDetEup	0.4
			IcePhL → EupS	fpPhLEup	1
			PhS → EupO	fpPhSEup	1
			PhL → EupO	fpPhLEup	1
			MZL → EupO	fpMZLEup	1
			Cop → EupO	fpCopEup	0.2
			Det → EupO	fpDetEupO	0

			DetF →	fpDetEupO	0
			EupO		
			IcePhL	fpPhLEup	1
			→ EupO		
			Cop →	fpCopJel	1
			Jel		
			NCaS →	fpNCaJel	1
			Jel		
			EupS →	fpEupJel	1
			Jel		
			NCaO	fpNCaJel	1
			→ Jel		
			EupO →	fpEupJel	1
			Jel		
			PhS →	prefPS	0.1
			Ben		
			PhL →	prefPL	1
			Ben		
			Det →	prefD	1
			Ben		
			DetF →	prefD	1
			Ben		
			DetBen	prefD	1
			→ Ben		
$e_Y$	maximum specific ingestion rate	$\text{mg}_{\text{Cprey}} \text{mg}_{\text{Cpred}}^{-1} \text{d}^{-1}$	MZL	eMZL	0.4
			Cop	eCop	0.4
			NCaS	eNCa	0.3
			NCaO	eNCa	0.3
			EupS	eEup	0.3
			EupO	eEup	0.3
			Jel	eJel	0.069
			Ben	Rup	0.05
$f_Y$	half-saturation constant for grazing	$\text{mg}_{\text{C}} \text{m}^{-3}$	MZL	fMZL	20
			Cop	fCop	30
			NCaS	fNCa	30
			NCaO	fNCa	30
			EupS	fEup	40
			EupO	fEup	40
		$\text{mg}_{\text{C}} \text{m}^{-2}$	Ben	KupP	10
			(pelagic food)		
			Ben	KupD	2000
			(benthic food)		
$Q_Y$	Q10 (rate change factor per 10 deg) for growth rate	--	MZL	Q10MLZ	2
			Cop	Q10Cop	1.7
			NCaS	Q10NCa	1.6
			NCaO	Q10NCa	1.6
			EupS	Q10Eup	1.5
			EupO	Q10Eup	1.5
			Jel	Q10Jele	2.4
			Ben	q10r	1.5
$Q_{TY}$	reference temperature for growth rate	°C	MZL	Q10MZLT	5
			Cop	Q10CopT	5
			NCaS	Q10NCaT	5
			NCaO	Q10NCaT	5
			EupS	Q10EupT	5
			EupO	Q10EupT	5
			Jel	Q10JelTe	10
			Ben	T0benr	5
$L_P$	threshold for benthos grazing	$\text{mg}_{\text{C}} \text{m}^{-2}$	Ben	LupP	1
			(pelagic food)		
$L_D$			Ben	LupD	292
			(benthic food)		

### 2.3.4 Egestion and excretion

Egestion fluxes associated with grazing and predation in the water column are a simple fraction of total prey eaten:

$$Ege(Y, Det[F])_k = (1 - \gamma_Y) \cdot \sum_Z Gra(Z, Y)_k \quad (42)$$

Egestion fluxes from the microzooplankton group (MZL) go to the slow-sinking detrital pool (Det); all other egestion fluxes go to the fast-sinking detrital pool (DetF).

Infauna egestion and excretion is a bit more complex; it is proportional to the prey eaten, with differing rates for detrital vs phytoplankton prey. The flux is split evenly, with half going to benthic detritus (BenDet) and half to NH4.

$$Exc(Ben, BenDet) = 0.5 \cdot \left( ex_D \cdot \sum_{X=det} Gra(X, Ben) + ex_P \cdot \sum_{X=phyto} Gra(X, Ben) \right) \quad (43)$$

$$Exc(Ben, NH4) = 0.5 \cdot \left( ex_D \cdot \sum_{X=det} Gra(X, Ben) + ex_P \cdot \sum_{X=phyto} Gra(X, Ben) \right) \quad (44)$$

As with benthic grazing, these benthic excretion fluxes are in units of mgC/m<sup>2</sup>/d. The flux to NH4 is assumed to return to the bottom water column layer, and is converted to a volumetric flux based on the thickness of that layer (see section 2.3.9).

**Table 7** – Notation and description for input parameters related to egestion and excretion.

Variable	Description	Units	Relevant input parameter(s)		
			Group	Parameter	Value
$\gamma_Y$	growth efficiency	--	MZL	gammaMZL	0.7
			Cop	gammaCop	0.7
			NCaS	gammaNCa	0.7
			NCaO	gammaNCa	0.7
			EupS (live prey)	gammaEup	0.7
			EupS (detrital prey)	hardcoded	0.3
			EupO (live prey)	gammaEup	0.7
			EupO (detrital prey)	hardcoded	0.3
			Jel	gammaJel	1
$ex_P$	excretion fraction (1 - growth efficiency)	--	Ben (living prey)	eex	0.3
			Ben (detrital prey)	eexD	0.5

### 2.3.5 Respiration

All pelagic producers and consumers except jellyfish respire following the temperature-dependent formulation of Arhonditsis & Brett (2005). The phytoplankton and microzooplankton groups maintain a constant basal metabolic rate ( $bm$ ):

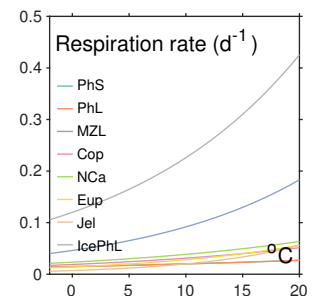
$$Res(X, NH4)_k = \exp(k_{tb} \cdot (T - T_{ref})) \cdot bm \cdot [X] \quad (45)$$

The larger zooplankton groups substitute a basal metabolic rate that includes a starvation response when prey is scarce:

$$Res(X, NH4)_k = \exp(k_{tb} \cdot (T - T_{ref})) \cdot B_{met} \cdot [X] \quad (46)$$

where

**Figure 8** – Respiration rates.



$$B_{met} = \begin{cases} bm \cdot \left( \frac{\sum_Z (fp_{ZY} \cdot [Z]^2)}{0.01} \right) & \sum_Z (fp_{ZY} \cdot [Z]^2) < 0.01 \\ bm & \text{otherwise} \end{cases} \quad (47)$$

(The summation relates to the total available prey; see [section 2.3.3](#) for details.)

The large copepod groups (NCaS and NCaO) also include a diapause adjustment, such that their basal metabolic rate  $bm$  is reduced to 10% of the  $bm$  parameter value during periods of downward migration. See [section 2.4](#) for details of the time-of-year calculation for diapause.

Jellyfish respiration also follows a temperature-dependent formula, after [Uye & Shimauchi \(2005\)](#):

$$Res(\text{Jel}, \text{NH4})_k = Q_r^{\left(\frac{T-Q_{Tr}}{10}\right)} \cdot bm \cdot [\text{Jel}] \quad (48)$$

Infaunal respiration includes terms for both basal metabolism and active metabolism proportional to grazing:

$$Res(\text{Ben}, \text{NH4}) = Q_B^{\left(\frac{T-Q_{TB}}{10}\right)} \cdot bm \cdot [\text{Ben}] + am \cdot \left( (1 - ex_D) \cdot \sum_{X=\text{det}} \text{Gra}(X, \text{Ben}) + (1 - ex_P) \cdot \sum_{X=\text{phyto}} \text{Gra}(X, \text{Ben}) \right) \quad (49)$$

Finally, ice algae respiration uses a metabolic rate linearly proportional to its maximum growth rate, after [Jin et al. \(2006\)](#):

$$Res(\text{IcePhL}, \text{IceNH4})_{ice} = r \cdot \mu_0 \cdot \exp(0.0633 \cdot T_{k=N}) \cdot [\text{IcePhL}] \quad (50)$$

As with ice algae production, the surface water temperature is used as a proxy for ice temperature when calculating the temperature component of this rate.

**Table 8** – Notation and description for input parameters related to respiration. (See [Table 6](#) for pelagic prey preferences and infauna Q-10 parameters, [Table 7](#) for infauna excretion fraction parameters, and [Table 5](#) for ice algae growth rate parameter.)

Variable	Description	Units	Relevant input parameter(s)					
			Group	Parameter	Value			
$bm$	basal metabolic rate	$d^{-1}$	PhS	respPhS	0.02			
			PhL	respPhL	0.02			
			MZL	respMZL	0.08			
			Cop	respCop	0.04			
			NCaS	respNca	0.03			
			NCaO	respNca	0.03			
			EupS	respEup	0.02			
			EupO	respEup	0.02			
			Jel	respJel	0.02			
			Ben	Rres	0.0027			
			$am$	active metabolic rate	$d^{-1}$	Ben	Qres	0.25
						$k_{tb}$	temperature coefficient for respiration	$^{\circ}\text{C}^{-1}$
			PhL	KtBm_PhL	0.03			
MZL	KtBm_MZL	0.069						
Cop	ktbmC	0.05						
NCaS	ktbmN	0.05						
NCaO	ktbmN	0.05						
EupS	ktbmE	0.069						

$T_{ref}$	reference temperature for respiration	°C	EupO	ktbmE	0.069
			PhS	TmaxPhS	10
			PhL	TmaxPhL	10
			MZL	TmaxMZL	8
			Cop	TrefC	15
			NCaS	TrefN	5
			NCaO	TrefN	5
			EupS	TrefE	5
			EupO	TrefE	5
			$Q_r$	Q10 for respiration rate	--
$Q_{Tr}$	reference temperature for Q10 respiration	°C	Jel	Q10JelTr	10
$r$	respiration rate as a fraction of maximum growth rate	--	IcePhL	R0i	0.05

### 2.3.6 Mortality and senescence

Non-predatory mortality losses for phytoplankton groups are formulated as a linear closure term:

$$Mor(X, Det)_k = m_L \cdot [X] \quad (51)$$

Microzooplankton losses have the option of following either a linear closure as above (MZLMOLIN flag defined), or a quadratic closure:

$$Mor(X, Det)_k = m_Q \cdot [X]^2 \quad (52)$$

Note that when switching between the linear and quadratic formulations, the relevant input parameter for the MZL group switches between `mMZL` and `mpredMZL`.

All larger zooplankton groups use a temperature-mediated quadratic closure term:

$$Mor(X, DetF)_k = Q_Y^{\left(\frac{T-Q_{TY}}{10}\right)} \cdot m_Q \cdot [X]^2 \quad (53)$$

Non-predatory mortality fluxes from the phytoplankton and microzooplankton groups go to the slow-sinking detritus, while all other non-predatory mortality losses go to the fast-sinking detritus.

The benthic infauna group includes both a linear and quadratic mortality function, the former to represent senescence and the latter as a predation closure term.

$$Mor(\text{Ben}, \text{BenDet}) = Q_B^{\left(\frac{T-Q_{TB}}{10}\right)} \cdot (m_L \cdot [\text{Ben}] + m_Q \cdot [\text{Ben}]^2) \quad (54)$$

Finally, ice algae use a linear mortality rate with a temperature dependence, following [Jin et al. \(2006\)](#):

$$Mor(\text{IcePhl}, \text{IceNH4})_{ice} = \exp(r_g \cdot T_{k=N}) \cdot m_{L0} \cdot [\text{IcePhL}] \quad (55)$$

**Table 9** – Notation and description for input parameters related to non-predatory mortality. (See [Table 6](#) for Q-10 parameters.)

Variable	Description	Units	Relevant input parameter(s)		
			Group	Parameter	Value
$m_L$	linear mortality rate	$\text{d}^{-1}$	PhS	mPhS	0.01
			PhL	mPhL	0.01
			Ben	rmort	0.0021
$m_Q$	quadratic mortality rate	$\text{mg}_C^{-1} \text{d}^{-1}$	MZL	mpredMZL	0.01
			Cop	mpredCop	0.05
			NCaS	mpredNCa	0.05

			NCaO	mpredNca	0.05
			EupS	mpredEup	0.05
			EupO	mpredEup	0.05
			Jel	mpredJel	0.006
			Ben	BenPred	$1 \times 10^{-6}$
$m_{L0}$	mortality rate at 0 deg C	$d^{-1}$	IcePhL	rg0	0.01
$r_g$	temperature coefficient for mortality	$^{\circ}C^{-1}$	IcePhL	rg	0.03

### 2.3.7 Remineralization and nitrification

Detrital remineralization is proportional to temperature and the nitrogen content of detritus, after Kawamiya et al. (2000):

$$Rem(X, NH4)_k = (P_{v0} \cdot \exp(P_{vT} \cdot T) \cdot [X] \cdot \xi) / \xi \quad (56)$$

The conversion from nitrogen content back to carbon content is done to maintain unit consistency with the other between-group fluxes, using the assumption that all living and detrital groups maintain identical C:N:Fe stoichiometry. Both fast- and slow-sinking detritus use the same parameters for this process.

Nitrification rate in the water column is also influenced by temperature (Arhonditsis & Brett, 2005):

$$Nit(NH4, NO3)_k = \left( n_0 \cdot \exp(-k_{tntr} \cdot (T - T_{opt})^2) \cdot [NH4] \cdot \frac{[NH4]}{k_{Nit} + [NH4]} \right) / \xi \quad (57)$$

Nitrification in the ice is a simple linear function of ammonium concentration (Jin et al., 2006):

$$Nit(IceNH4, IceNO3)_{ice} = (N_{nit} \cdot [IceNH4]) / \xi \quad (58)$$

As with remineralization, the final nitrification rate values are converted to carbon units simply for bookkeeping purposes; they will be converted back to nitrogen units when used in the final rate of change equations (see section 2.3.9.)

**Table 10** – Notation and description for input parameters related to remineralization and nitrification.

Variable	Description	Units	Relevant input parameter(s)		
			Group	Parameter	Value
$P_{v0}$	PON remineralization rate at 0 deg C	$d^{-1}$		Pv0	0.1
$P_{vT}$	temperature coefficient for remineralization	$^{\circ}C^{-1}$		PvT	0.069
$n_0$	nitrification rate at 0 deg C	$d^{-1}$		Nitr0	0.0107
$k_{tntr}$	temperature coefficient for nitrification	$^{\circ}C^{-1}$		ktntr	0.002
$T_{opt}$	optimal temperature for nitrification	$^{\circ}C$		ToptNit	20
$k_{Nit}$	half-saturation constant for nitrification	$mmol_N m^{-3}$		KNH4Nit	0.057
$N_{Nit}$	ice nitrification rate	$d^{-1}$		annit	0.0149

### 2.3.8 Ice interface convective exchange

Nitrate, ammonium, and large phytoplankton are exchanged between the ice layer and the surface water layer as a result of convective exchange of water and brine at the base of the ice. The rate of exchange of water is determined by the ice melt or ice growth rate following a polynomial fit to data as in Jin et al. (2006):

$$T_{wi} = \begin{cases} 720 \cdot 86400 \cdot \left( 4.9 \times 10^{-6} \cdot \left(-\frac{dH}{dt}\right) - 1.39 \times 10^{-5} \cdot \left(-\frac{dH}{dt}\right)^2 \right) & \frac{dH}{dt} \leq 0 \\ 72 \cdot 86400 \cdot \left( 9.667 \times 10^{-11} + 4.49 \times 10^{-6} \cdot \left(\frac{dH}{dt}\right) - 1.39 \times 10^{-5} \cdot \left(\frac{dH}{dt}\right)^2 \right) & \frac{dH}{dt} > 0 \end{cases} \quad (59)$$

where  $\frac{dH}{dt}$  is the rate of change of ice thickness ( $\text{m s}^{-1}$ ) between the current time step and the previous one. The resulting exchange rate,  $T_{wi}$ , is expressed in  $\text{m d}^{-1}$ .

The exchange in nutrients then becomes a function of the difference in concentrations in the surface layer of water versus the ice layer. Phytoplankton can be washed out of the skeletal ice layer but not in, so the exchange of ice algae and large phytoplankton assumes a concentration of 0 in the surface water:

$$T_{wi}(\text{IceNO}_3, \text{NO}_3) = T_{wi} \cdot ([\text{IceNO}_3] - [\text{NO}_3]) / \xi \quad (60)$$

$$T_{wi}(\text{IceNH}_4, \text{NH}_4) = T_{wi} \cdot ([\text{IceNH}_4] - [\text{NO}_3]) / \xi \quad (61)$$

$$T_{wi}(\text{IcePhL}, \text{PhL}) = T_{wi} \cdot [\text{IcePhL}] \quad (62)$$

This equation results in a rate of exchange of material across the boundary ( $\text{mgC}/\text{m}^2/\text{d}$ ) that can have either a positive value (net movement from ice to water) or a negative value (net movement from water to ice). As in previous sections, the nutrient transport is converted to carbon units here purely for bookkeeping purposes.

### 2.3.9 Total rate of change

The total rate of change for each state variable due to source-minus-sink processes is calculated as a sum of the rates detailed in the previous sections (section 2.3.2 – section 2.3.8). Recall that in the previous sections, all flux rates taking place within the pelagic water column layers, or within the ice layer, were expressed in volumetric units ( $\text{mgC}/\text{m}^3/\text{d}$ ), while all processes in the benthos or across the water-ice or water-benthos boundaries were expressed in per-area units ( $\text{mgC}/\text{m}^2/\text{d}$ ). Terms displayed in blue apply only in the top layer ( $k = N$ ), while terms displayed in brown apply only to the bottom layer ( $k = 1$ ).

$$\frac{d}{dt} \text{NO}_3_k = \left( \text{Nit}(\text{NH}_4, \text{NO}_3)_k - \sum_{\substack{X \in (\text{PhS}, \\ \text{PhL})}} G_{pp}(\text{NO}_3, X)_k + \frac{T_{wi}(\text{IceNO}_3, \text{NO}_3)}{h_k} \right) \cdot \xi \quad (63)$$

$$\begin{aligned} \frac{d}{dt} \text{NH}_4_k = & \left( \sum_{\substack{X \in (\text{PhS}, \\ \text{PhL}, \text{MZL}, \\ \text{Cop}, \text{NCaS}, \\ \text{NCaO}, \text{EupS}, \\ \text{EupO}, \text{Jel})}} \text{Res}(X, \text{NH}_4)_k + \sum_{\substack{X \in (\text{Det}, \\ \text{DetF})}} \text{Rem}(X, \text{NH}_4)_k - \sum_{\substack{X \in (\text{PhS}, \\ \text{PhL})}} G_{pp}(\text{NH}_4, X)_k \right. \\ & \left. - \text{Nit}(\text{NH}_4, \text{NO}_3)_k + \frac{\text{Exc}(\text{Ben}, \text{NH}_4)_k}{h_k} + \frac{\text{Res}(\text{Ben}, \text{NH}_4)_k}{h_k} + \frac{T_{wi}(\text{IceNH}_4, \text{NH}_4)_k}{h_k} \right) \cdot \xi \end{aligned} \quad (64)$$

$$\begin{aligned} \frac{d}{dt} \text{PhS}_k = & \sum_{\substack{X \in (\text{NO}_3, \\ \text{NH}_4)}} G_{pp}(X, \text{PhS})_k - \sum_{\substack{X \in (\text{MZL}, \\ \text{Cop}, \text{NCaS}, \\ \text{NCaO}, \text{EupS}, \\ \text{EupO})}} \text{Gra}(\text{PhS}, X)_k - \text{Mor}(\text{PhS}, \text{Det})_k - \text{Res}(\text{PhS}, \text{NH}_4)_k \\ & - \frac{\text{Gra}(\text{PhS}, \text{Ben}) \cdot w_{k, \text{PhS}}}{h_k} \end{aligned} \quad (65)$$

$$\begin{aligned} \frac{d}{dt} \text{PhL}_k &= \sum_{\substack{X \in (\text{NO}_3, \\ \text{NH}_4)}} Gpp(X, \text{PhL})_k - \sum_{\substack{X \in (\text{MZL}, \\ \text{Cop}, \text{NCaS}, \\ \text{NCaO}, \text{EupS}, \\ \text{EupO})}} Gra(\text{PhL}, X)_k - Mor(\text{PhL}, \text{Det})_k - Res(\text{PhL}, \text{NH}_4)_k \\ &\quad - \frac{Gra(\text{PhL}, \text{Ben}) \cdot w_{k, \text{PhL}}}{h_k} + \frac{Twil(\text{IcePhL}, \text{PhL})}{h_k} \end{aligned} \quad (66)$$

$$\begin{aligned} \frac{d}{dt} \text{MZL}_k &= \sum_{\substack{X \in (\text{PhS}, \\ \text{PhL})}} Gra(X, \text{MZL})_k - Ege(\text{MZL}, \text{Det})_k - \sum_{\substack{X \in (\text{Cop}, \\ \text{NCaS}, \text{NCaO}, \\ \text{EupS}, \text{EupO})}} Gra(\text{MZL}, X)_k \\ &\quad - Mor(\text{MZL}, \text{Det})_k - Res(\text{MZL}, \text{NH}_4)_k \end{aligned} \quad (67)$$

$$\begin{aligned} \frac{d}{dt} \text{Cop}_k &= \sum_{\substack{X \in (\text{PhS}, \\ \text{PhL}, \text{MZL}, \\ \text{IcePhL})}} Gra(X, \text{Cop})_k - Ege(\text{Cop}, \text{DetF})_k - \sum_{\substack{X \in (\text{EupS}, \\ \text{EupO}, \text{Jel})}} Gra(\text{Cop}, X)_k \\ &\quad - Mor(\text{Cop}, \text{DetF})_k - Res(\text{Cop}, \text{NH}_4)_k \end{aligned} \quad (68)$$

$$\begin{aligned} \frac{d}{dt} \text{NCaS}_k &= \sum_{\substack{X \in (\text{PhS}, \\ \text{PhL}, \text{MZL}, \\ \text{IcePhL})}} Gra(X, \text{NCaS})_k - Ege(\text{NCaS}, \text{DetF})_k - Gra(\text{NCaS}, \text{Jel})_k \\ &\quad - Mor(\text{NCaS}, \text{DetF})_k - Res(\text{NCaS}, \text{NH}_4)_k \end{aligned} \quad (69)$$

$$\begin{aligned} \frac{d}{dt} \text{EupS}_k &= \sum_{\substack{X \in (\text{PhS}, \\ \text{PhL}, \text{MZL}, \\ \text{Cop}, \text{IcePhL})}} Gra(X, \text{EupS})_k - Ege(\text{EupS}, \text{DetF})_k - Gra(\text{EupS}, \text{Jel})_k \\ &\quad - Mor(\text{EupS}, \text{DetF})_k - Res(\text{EupS}, \text{NH}_4)_k \end{aligned} \quad (70)$$

$$\begin{aligned} \frac{d}{dt} \text{NCaO}_k &= \sum_{\substack{X \in (\text{PhS}, \\ \text{PhL}, \text{MZL}, \\ \text{IcePhL})}} Gra(X, \text{NCaO})_k - Ege(\text{NCaO}, \text{DetF})_k - Gra(\text{NCaO}, \text{Jel})_k \\ &\quad - Mor(\text{NCaO}, \text{DetF})_k - Res(\text{NCaO}, \text{NH}_4)_k \end{aligned} \quad (71)$$

$$\begin{aligned} \frac{d}{dt} \text{EupO}_k &= \sum_{\substack{X \in (\text{PhS}, \\ \text{PhL}, \text{MZL}, \\ \text{Cop}, \text{IcePhL})}} Gra(X, \text{EupO})_k - Ege(\text{EupO}, \text{DetF})_k - Gra(\text{EupO}, \text{Jel})_k \\ &\quad - Mor(\text{EupO}, \text{DetF})_k - Res(\text{EupO}, \text{NH}_4)_k \end{aligned} \quad (72)$$

$$\begin{aligned} \frac{d}{dt} \text{Det}_k &= Ege(\text{MZL}, \text{Det})_k + \sum_{\substack{X \in (\text{PhS}, \\ \text{PhL}, \text{MZL})}} Mor(X, \text{Det})_k - \sum_{\substack{X \in (\text{EupS}, \\ \text{EupO})}} Gra(\text{Det}, X)_k - Rem(\text{Det}, \text{NH}_4)_k \\ &\quad - \frac{Gra(\text{Det}, \text{Ben}) \cdot w_{k, \text{Det}}}{h_k} \end{aligned} \quad (73)$$

$$\begin{aligned} \frac{d}{dt} \text{DetF}_k &= \sum_{\substack{X \in (\text{Cop}, \\ \text{NCaS}, \text{NCaO}, \\ \text{EupS}, \text{EupO}, \\ \text{Jel})}} Ege(X, \text{DetF})_k + \sum_{\substack{X \in (\text{Cop}, \\ \text{NCaS}, \text{NCaO}, \\ \text{EupS}, \text{EupO}, \\ \text{Jel})}} Mor(X, \text{DetF})_k - \sum_{\substack{X \in (\text{EupS}, \\ \text{EupO})}} Gra(\text{DetF}, X)_k \\ &\quad - Rem(\text{DetF}, \text{NH}_4)_k - \frac{Gra(\text{DetF}, \text{Ben}) \cdot w_{k, \text{DetF}}}{h_k} \end{aligned} \quad (74)$$

$$\begin{aligned} \frac{d}{dt} \text{Jel}_k &= \sum_{\substack{X \in (\text{Cop}, \\ \text{NCaS}, \text{NCaO}, \\ \text{EupS}, \text{EupO})}} Gra(X, \text{Jel})_k - Ege(\text{Jel}, \text{DetF})_k \\ &\quad - Mor(\text{Jel}, \text{DetF})_k - Res(\text{Jel}, \text{NH}_4)_k \end{aligned} \quad (75)$$

$$\frac{d}{dt} \text{Fe}_k = \left( \sum_{\substack{X \in (\text{PhS}, \\ \text{PhL})}} Gpp(\text{NO}_3, X)_k \right) \cdot FeC \quad (76)$$

$$\frac{d}{dt}\text{Ben} = \sum_{\substack{X \in (\text{Det}, \\ \text{DetF}, \text{PhS}, \\ \text{PhL}, \text{BenDet})}} \text{Gra}(X, \text{Ben}) - \sum_{\substack{X \in (\text{NH}_4, \\ \text{BenDet})}} \text{Exc}(\text{Ben}, X) - \text{Mor}(\text{Ben}, \text{BenDet}) - \text{Res}(\text{Ben}, \text{NH}_4) \quad (77)$$

$$\frac{d}{dt}\text{BenDet} = \text{Exc}(\text{Ben}, \text{BenDet}) + \text{Mor}(\text{Ben}, \text{BenDet}) - \text{Gra}(\text{BenDet}, \text{Ben}) - \text{Rem}(\text{BenDet}, \text{NH}_4) \quad (78)$$

$$\begin{aligned} \frac{d}{dt}\text{IcePhL} = & \sum_{\substack{X \in (\text{IceNO}_3, \\ \text{IceNH}_4)}} \text{Gpp}(X, \text{IcePhL})_{ice} - \left( \sum_{\substack{X \in (\text{Cop}, \\ \text{NCaS}, \text{NCaO}, \\ \text{EupS}, \text{EupO})}} \text{Gra}(\text{IcePhL}, X)_k \right) \cdot \frac{h_k}{h_{sice}} \\ & - \text{Mor}(\text{IcePhL}, \text{IceNH}_4)_{ice} - \text{Res}(\text{IcePhL}, \text{IceNH}_4)_{ice} - \frac{\text{Tw}i(\text{IcePhL}, \text{PhL})}{h_{sice}} \end{aligned} \quad (79)$$

$$\frac{d}{dt}\text{IceNO}_3 = \left( \text{Nit}(\text{IceNH}_4, \text{IceNO}_3)_{sice} - \text{Gpp}(\text{IceNO}_3, \text{IcePhL})_{ice} - \frac{\text{Tw}i(\text{IceNO}_3, \text{NO}_3)}{h_{sice}} \right) \cdot \xi \quad (80)$$

$$\begin{aligned} \frac{d}{dt}\text{IceNH}_4 = & (\text{Res}(\text{IcePhL}, \text{IceNH}_4)_{ice} + \text{Mor}(\text{IcePhL}, \text{IceNH}_4)_{ice} - \text{Gpp}(\text{IceNH}_4, \text{IcePhL})_{ice} \\ & - \text{Nit}(\text{IceNH}_4, \text{IceNO}_3)_{ice} - \frac{\text{Tw}i(\text{IceNH}_4, \text{NH}_4)}{h_{sice}}) \cdot \xi \end{aligned} \quad (81)$$

## 2.4 Vertical movement and exchanges

All vertical movement in the BEST\_NPZ model is calculated using a piecewise parabolic method and weighted non-oscillatory scheme, following the sediment settling code from a ROMS sediment model (Warner et al., 2008). This scheme allows for fast sinking speeds that may cause material to cross multiple layers, without being constrained by CFL criterion.

We have modified this scheme slightly to allow a zero-flux boundary condition to be imposed at a specified depth. We also allow the use of a vertical velocity rather sinking speed; a negative velocity implies sinking, while a positive velocity indicates rising.

### 2.4.1 Sinking of phytoplankton and detritus

Phytoplankton and detrital groups (PhS, PhL, Det, and DetF) are subject to vertical settling, with a constant sinking speed for each state variable.

When material crosses the water/benthic boundary, it is assumed that 20% of the material becomes biologically unavailable (Walsh et al., 1981; Walsh & McRoy, 1986), and 1% is lost to denitrification (pers. comm. with D. Schull via Gibson & Spitz, 2011). The remaining 79% of the flux across the boundary is transferred to the benthic detritus (BenDet.)

### 2.4.2 Copepod diapause

Copepod diapause is included in the BEST\_NPZ model by imposing seasonal movement through the water column on both large-bodied copepod groups (NCaS and NCaO), coupled with modifications to their feeding and respiration rates during periods of downward movement. The timing of copepod diapause is specified via input parameters for sinking start ( $S_{start}$ ), sinking end ( $S_{end}$ ), rising start ( $R_{start}$ ), and rising end ( $R_{end}$ ) day for each group, all specified as days of the year. These four parameters combine to define periods of downward directed movement ( $S_{start} \leq t_{doy} \leq S_{end}$ ), upward directed movement ( $R_{start} \leq t_{doy} \leq R_{end}$ ), and no directed movement ( $R_{end} < t_{doy} < S_{start}$  and  $S_{end} < t_{doy} < R_{start}$ ) (during all times, both groups are still subject to passive advection and diffusion).

Earlier versions allowed specification of  $S_{start}$ ,  $S_{end}$ ,  $R_{start}$ , and  $R_{end}$  for the off-shore group (NCaO) only, with the onshore group automatically lagged by 30 days behind the offshore group.

In the current version of the code, the 30-day lag is assumed when all four parameters are set to 0 for the on-shore group (this maintains backward-compatibility with older input files that do not include values for the on-shore group; BEST\_NPZ sets missing input parameters to zero by default). Diapause can be turned off for either group by setting all four timing parameters to the same non-zero value.

On-shore copepods migrate to 200 m depth during their diapause period. During downward movement, a zero-flux condition is set at 200 m or at the bottom boundary, whichever is shallower. When migrating upward, a zero-flux condition is applied to the top of the surface layer.

An alternative migration scheme for on-shelf large copepods is offered through the DEPTHLIMITER option<sup>12</sup>. If that is defined, NCaS in water greater than 200 m depth are considered to be outside their habitat; rather than imposing the no-flux boundary at 200 m, any NCaS that cross the 200 m boundary are instead assumed to die and transferred to the fast-sinking detritus (DetF) group. The numerics of this option may allow biomass to cross the bottom boundary; in this case the biomass is transferred from NCaS to BenDet.

<sup>12</sup> As with the other DEPTHLIMITER effects, I'd prefer to determine and implement the actual mechanism that prevents their survival off-shore rather than hitting them with an empirical death ray.

Offshore copepods migrate to 400 m depth for their diapause period. A zero-flux condition is set at 400 m. In shallower waters, any biomass that crosses the bottom boundary is transferred to the benthic detritus (BenDet) group. During upward movement, a zero-flux condition is applied to the top of the surface layer.

### 2.4.3 Euphausiid diel vertical migration

Diel vertical migration is currently implemented for on-shelf euphausiids through the (still experimental) EUPDIEL compilation flag. When defined, sinking and rising velocities are applied such that EupS move at a hard-coded speed of 100 m d<sup>-1</sup> toward a target depth, defined as the shallowest depth layer where photosynthetically active radiation ( $PAR \cdot I_0$ ) is less than 0.5 E/m<sup>2</sup>/d.

**Table 11** – Notation and description for input parameters related to vertical movement.

Variable	Description	Units	Relevant input parameter(s)		
			Group	Parameter	Value
$w$	sinking or rising speed	d <sup>-1</sup>	PhS	wPhS	0.05
			PhL	wPhL	1
			Det	wDet	1
			DetF	wDetF	10
			NCaS (down)	wNCsink	11
			NCaS (up)	wNCrise	12
			NCaO (down)	wNCsink	11
			NCaO (up)	wNCrise	12
$S_{start}$	start day of year for downward movement	day – of – year	NCaS	SinkStartCM	0
			NCaO	SinkStart	155
$S_{end}$	end day of year for downward movement	day – of – year	NCaS	SinkEndCM	0
			NCaO	SinkEnd	366
$R_{start}$	start day of year for upward movement	day – of – year	NCaS	RiseStartCM	0
			NCaO	RiseStart	0
$R_{end}$	end day of year for upward movement	day – of – year	NCaS	RiseEndCM	0
			NCaO	RiseEnd	60

## 2.5 Analytical relaxation of state variables

Iron concentrations throughout the water column are initialized using a vertical profile that prescribes values above 50 m and below 300 m, with a linear interpolation between these two depths. The values of the shallow- and deep-water limits are a function of the bottom depth

in a grid cell, with higher values in shallow water and lower values in deep water. The primary source of iron in this region is the sediment, and therefore this gradient between shallow and deep water is intended to capture the iron differences between on-shelf and off-shelf regions.

Iron-related biogeochemical processes are not included in this model. Instead, the iron state variable is continuously nudged towards these prescribed vertical profiles on an annual timescale. The nudging process is implemented using the generic ROMS framework for climatological nudging, with the TNUDG input parameter controlling the strength of the relaxation calculations.

**Table 12** – Notation and description for input parameters related to state variable nudging.

Variable	Description	Units	Relevant input parameter(s)		
			Group	Parameter	Value
	Surface value of iron in shallow water	$\mu\text{mol}_{\text{Fe}} \text{m}^{-3}$		Feinlo	2
	Below-mixed-layer value of iron in shallow water	$\mu\text{mol}_{\text{Fe}} \text{m}^{-3}$		Feinhi	4
	Surface value of iron in deep water	$\mu\text{mol}_{\text{Fe}} \text{m}^{-3}$		Feofflo	0.01
	Below-mixed-layer value of iron in deep water	$\mu\text{mol}_{\text{Fe}} \text{m}^{-3}$		Feoffhi	2
	Bottom depth corresponding to shallow water values	m		Feinh	20
	Bottom depth corresponding to deep values	m		Feoffh	100
	relaxation time interval for iron	d		TNUDG (iFe)	360

### 3 Compilation flags

Within the ROMS source code, C preprocessing flags are used to selectively compile the code. Several C preprocessing flags appear throughout the BEST\_NPZ code; those that currently exist in the master branch of the source code are detailed in the following table.

A few of these compilation options resulted from the gradual addition of new features (such as the addition of benthic and ice state variables) that later became, for all intents and purposes, permanent additions to the BEST\_NPZ model. These are noted in the table as "recommended to always define." While we have attempted to keep the source code flexible to all compilation options, we rarely even test for compilation stability with these undefined, and all recent model validation work assumes these model features are present.

**Table 13** – Compilation flags related to the BEST\_NPZ model.

Compilation flag	Purpose	Notes
BENTHIC	Turns on benthic portion of the module. This adds the Ben and BenDet variables along with all associated flux processes.	Advised to always define with BEST_NPZ; not often tested without benthos.
BERING_10K	ROMS application flag for Bering 10K domain. Also used in many parts of the ice code as shorthand for "use variables from ice model" (as opposed to analytical one-dimensional ice)	
CLIM_ICE_1D	Use analytical calculations for a seasonal ice cycle (typically used when no full ice model is coupled to the physical model, as in one-dimensional simulations)	
CORRECT_TEMP_BIAS	Subtracts 1.94°C from water temperature for biological rate calculations	Legacy... not sure when or where this bias-correction was needed.
DEPTHLIMITER	Switch to turn on on/off-shelf enforcers for NCa and Eup groups	Provided for consistency with ggibson branch, but not recommended
DIAPAUSE	Turn on copepod diapause (vertical movement with accompanying reductions in feeding and respiration)	Recommended to always define. Behavior can now be turned off for individual simulations through use of input parameters without the need to recompile.
DIURNAL_SRFLUX	Sets day length (a now-unused internal parameter) to 24 hours rather than a latitude-and-declination calculation	
EUPDIEL	Turn on euphausiid diel vertical migration	Still experimental
FEAST	Turns on the FEAST upper trophic level model	Not documented here; requires a large number of additional input variables and parameters.
FEAST_NOEXCHANGE		

GPPMID	Calculate gross primary production at midpoint of layer, rather than integrating nonlinear processes over the layer.	Usually defined. The integrate-over-layer option performed marginally better in deep water when using a coarse 10-layer depth resolution. However, increasing the vertical resolution and sticking with the typical midpoint calculations proved to be a much better solution.
ICE_BIO	Turn on ice biology. This adds the IcePhL, IceNO3, and IceNH4 variables and all related fluxes	Advised to always define with BEST_NPZ; not often tested without ice biology. Also, must define either CLIM_ICE_1D or BERING_10K to work.
IRON_LIMIT	Turn on iron limitation. This adds the Fe variable and all associated fluxes.	Advised to always define with BEST_NPZ; not often tested without iron limitation.
JELLY	Turn on jellyfish. This adds the Jel variable and all associated fluxes.	Advised to always define with BEST_NPZ; not often tested without jellyfish.
LINEAR_CONTINUATION	An option in the sinking code subfunction (used for particle sinking and diapause) related to the WENO scheme. Inherited from sediment sinking code.	
MATLAB_COMPILE	Modify biology_tile subroutine for standalone compilation	This flag should never be defined when running a full ROMS simulation; intended for my Matlab-based unit-testing environment (allows the file to be compiled as a Matlab mex-Fortran file).
MZLMOLIN	Switch to linear form for MZL non-predatory mortality (quadratic otherwise)	
NEUMANN	An option in the sinking code subfunction (used for particle sinking and diapause) related to the WENO scheme. Inherited from sediment sinking code.	
PI_CONSTANT	Use a constant value (provided as an input parameter) for the $\alpha$ parameter when calculating the photosynthesis-irradiance curve (see <a href="#">section 2.3.2</a> ).	Recommended for now... variable- $\alpha$ equation is a bit questionable.
SPINUPBIO	Run the model in biological spinup mode, starting with only deep nitrate (at $40 \text{ mmol}_N \text{ m}^{-3}$ below 300 m).	Only relevant if ANA_BIOLOGY is defined.
STATIONARY	Calculate 3D stationary diagnostic variables.	
STATIONARY2	Calculate 2D stationary diagnostic variables.	Currently a placeholder, but available if we need any 2D diagnostics
fixedPRED		Legacy; do not define.

---

Flags not specific to BEST\_NPZ but found in the bestnpz.h source code

---

ASSUMED_SHAPE	
DISTRIBUTE	Internal switch to run in parallel
EW_PERIODIC	Use east-west periodic boundary conditions

MASKING	Use land/sea masking
NS_PERIODIC	Use north-south periodic boundary conditions
PROFILE	Use time profiling
TS_MPDATA	Use MPDATA finite difference solver for 3D advective time-stepping

---

## 4 Output variables

The BEST\_NPZ module allows for a large number of variables to be added to the various ROMS output files (history, average, and station files).

Regardless of compilation options, the biological tracer variables are saved and available as output variables. Water column tracers are specified via the H/Sout (idTvar) input parameters. The exact tracer variables available, and their positions within the idTvar array, depend on whether the ICE\_BIO, BENTHIC, IRON\_LIMIT, and JELLY compilation flags are defined; see Table 14 for details. Benthic tracers can be specified for output through the H/Sout (idBvar) input; iBen = 1 and iDetBen = 2 within this array. The ice variables are turned on and off with the variable-specific input parameters H/Sout (idIcePhL), H/Sout (idIceNO3), and H/Sout (idIceNH4).

**Table 14** – Indices in the idTvar array. Note that Hout (idTvar) appears separately in the ocean.in file and BPARNAM file, with the latter including only biological active tracers. The Sout (idTvar) input appears only once, in the STANAME file, and biological tracer indices begin at NAT+1; NAT is here assumed to be 2, for temperature and salinity. In all cases, note the skip between iPhL and iMZL due to the now-deprecated small microzooplankton group.

Index	Hout (in BPARNAM file)				Sout			
	none	JELLY	IRON_LIMIT	both	none	JELLY	IRON_LIMIT	both
iNO3	1	1	1	1	3	3	3	3
iNH4	2	2	2	2	4	4	4	4
iPhS	3	3	3	3	5	5	5	5
iPhL	4	4	4	4	6	6	6	6
iMZL	6	6	6	6	8	8	8	8
iCop	7	7	7	7	9	9	9	9
iNCaS	8	8	8	8	10	10	10	10
iEupS	9	9	9	9	11	11	11	11
iNCaO	10	10	10	10	12	12	12	12
iEupO	11	11	11	11	13	13	13	13
iDet	12	12	12	12	14	14	14	14
iDetF	13	13	13	13	15	15	15	15
iJel	–	14	–	14	–	16	–	16
iFe	–	–	14	15	–	–	16	17

If the STATIONARY flag is defined, many more intermediate diagnostic variables are saved internally and available for output. These are controlled by the idTSvar index array to Hout and Sout. Note that when running with a subdivided timestep (BioIter > 1), these diagnostic variables will reflect the values calculated during the final subdivision only.

Older versions of the code included a second compilation flag, STATIONARY2 (with the corresponding index array idTS2var), to define two-dimensional stationary diagnostics. In my rewrite, I did not end up requiring any 2D diagnostics. However, the code structure is still in place for this if we decided to use it in the future.

See Table 16 for a comprehensive description of all output variables associated with the BEST\_NPZ model.

**Table 16** – Output variables available in the BEST\_NPZ and FEAST models.

Index	Short name	Long name	Variable type
idTvar (iNO3)	NO3	Nitrate concentration	3D RHO-variable
idTvar (iNH4)	NH4	Ammonium concentration	3D RHO-variable
idTvar (iPhS)	PhS	Small phytoplankton concentration	3D RHO-variable
idTvar (iPhL)	PhL	Large phytoplankton concentration	3D RHO-variable
idTvar (iMZL)	MZL	Microzooplankton concentration	3D RHO-variable

idTvar (iCop)	Cop	Small copepod concentration	3D RHO-variable
idTvar (iNCaS)	NCaS	On-shelf large copepod concentration	3D RHO-variable
idTvar (iEupS)	EupS	On-shelf euphausiid concentration	3D RHO-variable
idTvar (iNCaO)	NCaO	Offshore large copepod concentration	3D RHO-variable
idTvar (iEupO)	EupO	Offshore euphausiid concentration	3D RHO-variable
idTvar (iDet)	Det	Slow-sinking detritus concentration	3D RHO-variable
idTvar (iDetF)	DetF	Fast-sinking detritus concentration	3D RHO-variable
idTvar (iJel)	Jel	Jellyfish concentration	3D RHO-variable
idBvar (iBen)	Ben	Benthic infauna concentration	2D RHO-variable
idBvar (iDetBen)	DetBen	Benthic detritus concentration	2D RHO-variable
idIcePhL	IcePhL	Ice algae concentration	2D RHO-variable
idIceNO3	IceNO3	Ice nitrate concentration	2D RHO-variable
idIceNH4	IceNH4	Ice ammonium concentration	2D RHO-variable
idTSvar (i3Stat1)	LightLimS	PhS Light limitation	3D RHO-variable
idTSvar (i3Stat2)	LightLimL	PhL Light limitation	3D RHO-variable
idTSvar (i3Stat3)	NOLimS	PhS NO3 limitation	3D RHO-variable
idTSvar (i3Stat4)	NOLimL	PhL NO3 limitation	3D RHO-variable
idTSvar (i3Stat5)	NHLimS	PhS NH4 limitation	3D RHO-variable
idTSvar (i3Stat6)	NHLimL	PhL NH4 limitation	3D RHO-variable
idTSvar (i3Stat7)	IronLimS	PhS Iron limitation	3D RHO-variable
idTSvar (i3Stat8)	IronLimL	PhL Iron limitation	3D RHO-variable
idTSvar (i3Stat9)	Gpp_NO3_PhS	gross primary production flux from NO3 to PhS	3D RHO-variable
idTSvar (i3Stat10)	Gpp_NO3_PhL	gross primary production flux from NO3 to PhL	3D RHO-variable
idTSvar (i3Stat11)	Gpp_NH4_PhS	gross primary production flux from NH4 to PhS	3D RHO-variable
idTSvar (i3Stat12)	Gpp_NH4_PhL	gross primary production flux from NH4 to PhL	3D RHO-variable
idTSvar (i3Stat13)	Gra_PhS_MZL	grazing/predation flux from PhS to MZL	3D RHO-variable
idTSvar (i3Stat14)	Gra_PhL_MZL	grazing/predation flux from PhL to MZL	3D RHO-variable
idTSvar (i3Stat15)	Ege_MZL_Det	egestion flux from MZL to Det	3D RHO-variable
idTSvar (i3Stat16)	Gra_PhS_Cop	grazing/predation flux from PhS to Cop	3D RHO-variable
idTSvar (i3Stat17)	Gra_PhL_Cop	grazing/predation flux from PhL to Cop	3D RHO-variable
idTSvar (i3Stat18)	Gra_MZL_Cop	grazing/predation flux from MZL to Cop	3D RHO-variable
idTSvar (i3Stat19)	Gra_IPhL_Cop	grazing/predation flux from IcePhL to Cop	3D RHO-variable
idTSvar (i3Stat20)	Ege_Cop_DetF	egestion flux from Cop to DetF	3D RHO-variable
idTSvar (i3Stat21)	Gra_PhS_NCaS	grazing/predation flux from PhS to NCaS	3D RHO-variable
idTSvar (i3Stat22)	Gra_PhL_NCaS	grazing/predation flux from PhL to NCaS	3D RHO-variable
idTSvar (i3Stat23)	Gra_MZL_NCaS	grazing/predation flux from MZL to NCaS	3D RHO-variable
idTSvar (i3Stat24)	Gra_IPhL_NCaS	grazing/predation flux from IcePhL to NCaS	3D RHO-variable
idTSvar (i3Stat25)	Ege_NCaS_DetF	egestion flux from NCaS to DetF	3D RHO-variable
idTSvar (i3Stat26)	Gra_PhS_NCaO	grazing/predation flux from PhS to NCaO	3D RHO-variable
idTSvar (i3Stat27)	Gra_PhL_NCaO	grazing/predation flux from PhL to NCaO	3D RHO-variable
idTSvar (i3Stat28)	Gra_MZL_NCaO	grazing/predation flux from MZL to NCaO	3D RHO-variable

idTSvar (i3Stat29)	Gra_IPhL_NCaO	grazing/predation flux from IcePhL to NCaO	3D RHO-variable
idTSvar (i3Stat30)	Ege_NCaO_DetF	egestion flux from NCaO to DetF	3D RHO-variable
idTSvar (i3Stat31)	Gra_PhS_EupS	grazing/predation flux from PhS to EupS	3D RHO-variable
idTSvar (i3Stat32)	Gra_PhL_EupS	grazing/predation flux from PhL to EupS	3D RHO-variable
idTSvar (i3Stat33)	Gra_MZL_EupS	grazing/predation flux from MZL to EupS	3D RHO-variable
idTSvar (i3Stat34)	Gra_Cop_EupS	grazing/predation flux from Cop to EupS	3D RHO-variable
idTSvar (i3Stat35)	Gra_IPhL_EupS	grazing/predation flux from IcePhL to EupS	3D RHO-variable
idTSvar (i3Stat36)	Gra_Det_EupS	grazing/predation flux from Det to EupS	3D RHO-variable
idTSvar (i3Stat37)	Gra_DetF_EupS	grazing/predation flux from DetF to EupS	3D RHO-variable
idTSvar (i3Stat38)	Ege_EupS_DetF	egestion flux from EupS to DetF	3D RHO-variable
idTSvar (i3Stat39)	Gra_PhS_EupO	grazing/predation flux from PhS to EupO	3D RHO-variable
idTSvar (i3Stat40)	Gra_PhL_EupO	grazing/predation flux from PhL to EupO	3D RHO-variable
idTSvar (i3Stat41)	Gra_MZL_EupO	grazing/predation flux from MZL to EupO	3D RHO-variable
idTSvar (i3Stat42)	Gra_Cop_EupO	grazing/predation flux from Cop to EupO	3D RHO-variable
idTSvar (i3Stat43)	Gra_IPhL_EupO	grazing/predation flux from IcePhL to EupO	3D RHO-variable
idTSvar (i3Stat44)	Gra_Det_EupO	grazing/predation flux from Det to EupO	3D RHO-variable
idTSvar (i3Stat45)	Gra_DetF_EupO	grazing/predation flux from DetF to EupO	3D RHO-variable
idTSvar (i3Stat46)	Ege_EupO_DetF	egestion flux from EupO to DetF	3D RHO-variable
idTSvar (i3Stat47)	Gra_Cop_Jel	grazing/predation flux from Cop to Jel	3D RHO-variable
idTSvar (i3Stat48)	Gra_EupS_Jel	grazing/predation flux from EupS to Jel	3D RHO-variable
idTSvar (i3Stat49)	Gra_EupO_Jel	grazing/predation flux from EupO to Jel	3D RHO-variable
idTSvar (i3Stat50)	Gra_NCaS_Jel	grazing/predation flux from NCaS to Jel	3D RHO-variable
idTSvar (i3Stat51)	Gra_NCaO_Jel	grazing/predation flux from NCaO to Jel	3D RHO-variable
idTSvar (i3Stat52)	Ege_Jel_DetF	egestion flux from Jel to DetF	3D RHO-variable
idTSvar (i3Stat53)	Mor_PhS_Det	other mortality flux from PhS to Det	3D RHO-variable
idTSvar (i3Stat54)	Mor_PhL_Det	other mortality flux from PhL to Det	3D RHO-variable
idTSvar (i3Stat55)	Mor_MZL_Det	other mortality flux from MZL to Det	3D RHO-variable
idTSvar (i3Stat56)	Mor_Cop_DetF	other mortality flux from Cop to DetF	3D RHO-variable
idTSvar (i3Stat57)	Mor_NCaS_DetF	other mortality flux from NCaS to DetF	3D RHO-variable
idTSvar (i3Stat58)	Mor_EupS_DetF	other mortality flux from EupS to DetF	3D RHO-variable
idTSvar (i3Stat59)	Mor_NCaO_DetF	other mortality flux from NCaO to DetF	3D RHO-variable
idTSvar (i3Stat60)	Mor_EupO_DetF	other mortality flux from EupO to DetF	3D RHO-variable
idTSvar (i3Stat61)	Mor_Jel_DetF	other mortality flux from Jel to DetF	3D RHO-variable
idTSvar (i3Stat62)	Res_PhS_NH4	respiration flux from PhS to NH4	3D RHO-variable
idTSvar (i3Stat63)	Res_PhL_NH4	respiration flux from PhL to NH4	3D RHO-variable
idTSvar (i3Stat64)	Res_MZL_NH4	respiration flux from MZL to NH4	3D RHO-variable

idTSvar (i3Stat65)	Res_Cop_NH4	respiration flux from Cop to NH4	3D RHO-variable
idTSvar (i3Stat66)	Res_NCaS_NH4	respiration flux from NCaS to NH4	3D RHO-variable
idTSvar (i3Stat67)	Res_NCaO_NH4	respiration flux from NCaO to NH4	3D RHO-variable
idTSvar (i3Stat68)	Res_EupS_NH4	respiration flux from EupS to NH4	3D RHO-variable
idTSvar (i3Stat69)	Res_EupO_NH4	respiration flux from EupO to NH4	3D RHO-variable
idTSvar (i3Stat70)	Res_Jel_NH4	respiration flux from Jel to NH4	3D RHO-variable
idTSvar (i3Stat71)	Rem_Det_NH4	reminalization flux from Det to NH4	3D RHO-variable
idTSvar (i3Stat72)	Rem_DetF_NH4	reminalization flux from DetF to NH4	3D RHO-variable
idTSvar (i3Stat73)	Nit_NH4_NO3	nitrification flux from NH4 to NO3	3D RHO-variable
idTSvar (i3Stat74)	Gra_Det_Ben	grazing/predation flux from Det to Ben	3D RHO-variable
idTSvar (i3Stat75)	Gra_DetF_Ben	grazing/predation flux from DetF to Ben	3D RHO-variable
idTSvar (i3Stat76)	Gra_PhS_Ben	grazing/predation flux from PhS to Ben	3D RHO-variable
idTSvar (i3Stat77)	Gra_PhL_Ben	grazing/predation flux from PhL to Ben	3D RHO-variable
idTSvar (i3Stat78)	Gra_DetBen_Ben	grazing/predation flux from DetBen to Ben	3D RHO-variable
idTSvar (i3Stat79)	Exc_Ben_NH4	excretion flux from Ben to NH4	3D RHO-variable
idTSvar (i3Stat80)	Exc_Ben_DetBen	excretion flux from Ben to DetBen	3D RHO-variable
idTSvar (i3Stat81)	Res_Ben_NH4	respiration flux from Ben to NH4	3D RHO-variable
idTSvar (i3Stat82)	Mor_Ben_DetBen	other mortality flux from Ben to DetBen	3D RHO-variable
idTSvar (i3Stat83)	Rem_DetBen_NH4	reminalization flux from DetBen to NH4	3D RHO-variable
idTSvar (i3Stat84)	Gpp_INO3_IPhL	gross primary production flux from IceNO3 to IcePhL	3D RHO-variable
idTSvar (i3Stat85)	Gpp_INH4_IPhL	gross primary production flux from IceNH4 to IcePhL	3D RHO-variable
idTSvar (i3Stat86)	Res_IPhL_INH4	respiration flux from IcePhL to IceNH4	3D RHO-variable
idTSvar (i3Stat87)	Mor_IPhL_INH4	other mortality flux from IcePhL to IceNH4	3D RHO-variable
idTSvar (i3Stat88)	Nit_INH4_INO3	nitrification flux from IceNH4 to IceNO3	3D RHO-variable
idTSvar (i3Stat89)	Twi_IPhL_PhL	ice/water exchange flux from IcePhL to PhL	3D RHO-variable
idTSvar (i3Stat90)	Twi_INO3_NO3	ice/water exchange flux from IceNO3 to NO3	3D RHO-variable
idTSvar (i3Stat91)	Twi_INH4_NH4	ice/water exchange flux from IceNH4 to NH4	3D RHO-variable
idTSvar (i3Stat92)	Ver_PhS_DetBen	sinking-to-bottom flux from PhS to DetBen	3D RHO-variable
idTSvar (i3Stat93)	Ver_PhS_Out	sinking-to-bottom flux from PhS to Out	3D RHO-variable
idTSvar (i3Stat94)	Ver_PhL_DetBen	sinking-to-bottom flux from PhL to DetBen	3D RHO-variable
idTSvar (i3Stat95)	Ver_PhL_Out	sinking-to-bottom flux from PhL to Out	3D RHO-variable
idTSvar (i3Stat96)	Ver_Det_DetBen	sinking-to-bottom flux from Det to DetBen	3D RHO-variable
idTSvar (i3Stat97)	Ver_Det_Out	sinking-to-bottom flux from Det to Out	3D RHO-variable
idTSvar (i3Stat98)	Ver_DetF_DetBen	sinking-to-bottom flux from DetF to DetBen	3D RHO-variable
idTSvar (i3Stat99)	Ver_DetF_Out	sinking-to-bottom flux from DetF to Out	3D RHO-variable

idTSvar (i3Stat100)	Ver_NCaO_DetBen	sinking-to-bottom flux from NCaO to DetBen	3D RHO-variable
idTSvar (i3Stat101)	Ver_NCaS_DetF	sinking-to-bottom flux from NCaS to DetF	3D RHO-variable
idTSvar (i3Stat102)	Ver_NCaS_DetBen	sinking-to-bottom flux from NCaS to DetBen	3D RHO-variable
idTSvar (i3Stat103)	Frz_PhL_IPhL	freezing(+)/melting(-) flux from PhL to IcePhL	3D RHO-variable
idTSvar (i3Stat104)	Frz_NO3_INO3	freezing(+)/melting(-) flux from NO3 to IceNO3	3D RHO-variable
idTSvar (i3Stat105)	Frz_NH4_INH4	freezing(+)/melting(-) flux from NH4 to IceNH4	3D RHO-variable
idTSvar (i3Stat106)	prod_PhS	PhS net production rate	3D RHO-variable
idTSvar (i3Stat107)	prod_PhL	PhL net production rate	3D RHO-variable
idTSvar (i3Stat108)	prod_MZL	MZL net production rate	3D RHO-variable
idTSvar (i3Stat109)	prod_Cop	Cop net production rate	3D RHO-variable
idTSvar (i3Stat110)	prod_NCaS	NCaS net production rate	3D RHO-variable
idTSvar (i3Stat111)	prod_EupS	EupS net production rate	3D RHO-variable
idTSvar (i3Stat112)	prod_NCaO	NCaO net production rate	3D RHO-variable
idTSvar (i3Stat113)	prod_EupO	EupO net production rate	3D RHO-variable
idTSvar (i3Stat114)	prod_Jel	Jel net production rate	3D RHO-variable
idTSvar (i3Stat115)	prod_Ben	Ben net production rate	3D RHO-variable
idTSvar (i3Stat116)	prod_IcePhL	IcePhL net production rate	3D RHO-variable
idTSvar (i3Stat117)	onExit_NO3	NO3 biomass tracker	3D RHO-variable
idTSvar (i3Stat118)	onExit_NH4	NH4 biomass tracker	3D RHO-variable
idTSvar (i3Stat119)	onExit_PhS	PhS biomass tracker	3D RHO-variable
idTSvar (i3Stat120)	onExit_PhL	PhL biomass tracker	3D RHO-variable
idTSvar (i3Stat121)	onExit_MZL	MZL biomass tracker	3D RHO-variable
idTSvar (i3Stat122)	onExit_Cop	Cop biomass tracker	3D RHO-variable
idTSvar (i3Stat123)	onExit_NCaS	NCaS biomass tracker	3D RHO-variable
idTSvar (i3Stat124)	onExit_EupS	EupS biomass tracker	3D RHO-variable
idTSvar (i3Stat125)	onExit_NCaO	NCaO biomass tracker	3D RHO-variable
idTSvar (i3Stat126)	onExit_EupO	EupO biomass tracker	3D RHO-variable
idTSvar (i3Stat127)	onExit_Det	Det biomass tracker	3D RHO-variable
idTSvar (i3Stat128)	onExit_DetF	DetF biomass tracker	3D RHO-variable
idTSvar (i3Stat129)	onExit_Jel	Jel biomass tracker	3D RHO-variable
idTSvar (i3Stat130)	onExit_Fe	Fe biomass tracker	3D RHO-variable
idTSvar (i3Stat131)	advdiff_NO3	NO3 rate of change due to advection and diffusion	3D RHO-variable
idTSvar (i3Stat132)	advdiff_NH4	NH4 rate of change due to advection and diffusion	3D RHO-variable
idTSvar (i3Stat133)	advdiff_PhS	PhS rate of change due to advection and diffusion	3D RHO-variable
idTSvar (i3Stat134)	advdiff_PhL	PhL rate of change due to advection and diffusion	3D RHO-variable
idTSvar (i3Stat135)	advdiff_MZL	MZL rate of change due to advection and diffusion	3D RHO-variable
idTSvar (i3Stat136)	advdiff_Cop	Cop rate of change due to advection and diffusion	3D RHO-variable
idTSvar (i3Stat137)	advdiff_NCaS	NCaS rate of change due to advection and diffusion	3D RHO-variable
idTSvar (i3Stat138)	advdiff_EupS	EupS rate of change due to advection and diffusion	3D RHO-variable

idTSvar (i3Stat139)	advdiff_NCaO	NCaO rate of change due to advection and diffusion	3D RHO-variable
idTSvar (i3Stat140)	advdiff_EupO	EupO rate of change due to advection and diffusion	3D RHO-variable
idTSvar (i3Stat141)	advdiff_Det	Det rate of change due to advection and diffusion	3D RHO-variable
idTSvar (i3Stat142)	advdiff_DetF	DetF rate of change due to advection and diffusion	3D RHO-variable
idTSvar (i3Stat143)	advdiff_Jel	Jel rate of change due to advection and diffusion	3D RHO-variable
idTSvar (i3Stat144)	advdiff_Fe	Fe rate of change due to advection and diffusion	3D RHO-variable
idTSvar (i3Stat145)	feastpred_Cop	Cop cumulative daily predation loss to fish	3D RHO-variable
idTSvar (i3Stat146)	feastpred_NCaS	NCaS cumulative daily predation loss to fish	3D RHO-variable
idTSvar (i3Stat147)	feastpred_NCaO	NCaO cumulative daily predation loss to fish	3D RHO-variable
idTSvar (i3Stat148)	feastpred_EupS	EupS cumulative daily predation loss to fish	3D RHO-variable
idTSvar (i3Stat149)	feastpred_EupO	EupO cumulative daily predation loss to fish	3D RHO-variable

---

## 5 Internal dynamics of the BEST-NPZ model in the Bering Sea

The biological processes detailed in [section 2](#) operate across a wide range of time spans. Many of the processes related to the pelagic water column operate on time scales of a few days. In this model (and in most traditional nutrient-phytoplankton-zooplankton-detritus models), these processes, such as pelagic primary and secondary production, are relatively oblivious to their initial conditions. Even given wildly inaccurate starting points, most of the biological state variables will quickly rise or fall to their internally-regulated seasonal cycle.

However, the introduction of the longer-timescale benthic variables in this particular model, coupled with the geometry and circulation patterns of the Bering Sea shelf, lead to a much longer spinup time required for a Bering Sea BEST\_NPZ simulation to reach an internally-regulated equilibrium state.

Here, we provide the results of a 50-year spinup simulation. This simulation provides some insight into the mean state variable values that result from the balance of flux processes within the BEST-NPZ model. The values of all biological state variables at the conclusion of this simulation can also be used as baseline initial conditions for future experiments, allowing us to isolate the effects of intentional perturbations to the model forcing from any long-term drift due to initialization mismatch.

We present these results with minimal discussion, since this is intended only as a demonstration of the values resulting from the model equations and parameterizations detailed in the previous sections, not as a critique of the model's skill.

These simulations couple the BEST\_NPZ module to the ROMS Bering 10K domain. This model domain spans the entire Bering Sea shelf with 10-km horizontal resolution and 30 surface-following depth layers ([Figure 9](#)). Surface forcings repeat the 2001 values from the Climate Forecast System Operational Analysis (CFSv2) dataset ([Saha et al., 2010](#)); bulk forcings were used to relate winds, air temperature, specific humidity, surface pressure, and shortwave and longwave radiation from this dataset to surface stress and heat fluxes. The year 2001 was chosen because it represents a relatively average ice year. Lateral boundary conditions for the open southern and eastern boundaries of the model domain use a hybrid nudging/radiation scheme ([Marchesiello et al., 2001](#)), with physical values also derived from the CFSv2 dataset. Lateral boundary conditions for nitrate and ammonium use a monthly climatology<sup>13</sup>, while all other biological state variable boundary condition values are set to zero. The northern boundary enforces a fixed outflow through the Bering Strait of 0.8 Sv. Freshwater runoff due to river input derives from a historical reconstruction of streamflow [Kearney, in press]; river input is distributed as a surface freshwater flux based on river mouth location, with an e-folding scale of 20 km.

Physical variables for this simulation are initialized from the Jan 1, 2001 values of a previous hindcast of the Bering10K domain<sup>14</sup>. Nitrate was initialized to a constant value of 40 mmolN/m<sup>3</sup> below 50 m, transitioning to 0 mmolN/m<sup>3</sup> at 30 m. Iron was initialized to a depth-dependent profile as described in [section 2.5](#). All living biological state variables (i.e. phytoplankton, zooplankton, and benthic infauna) were initialized using a tiny seed value to allow future growth, while the remaining state variables were initialized at zero.

Note: the following figures are a work in progress. The eventual intent is to show values across the domain; for now, I'm just showing a few selected locations.

<sup>13</sup> This climatology dates back to the earliest runs of the Bering10K model domain, and its origin is unclear. Perhaps it was derived from previous simulations of the larger NEP domain?

<sup>14</sup> ...which itself was initialized from a previous run of the larger Northeast Pacific (NEP) ROMS domain, which initialized from SODA reanalysis ([Carton & Giese, 2008](#)). The spinup effects of a physics-only (i.e. no biological module turned on) run in this particular domain are usually resolved within a year or two ([Danielson et al., 2011](#)), so we decided not to worry too much about the provenance of these initial values

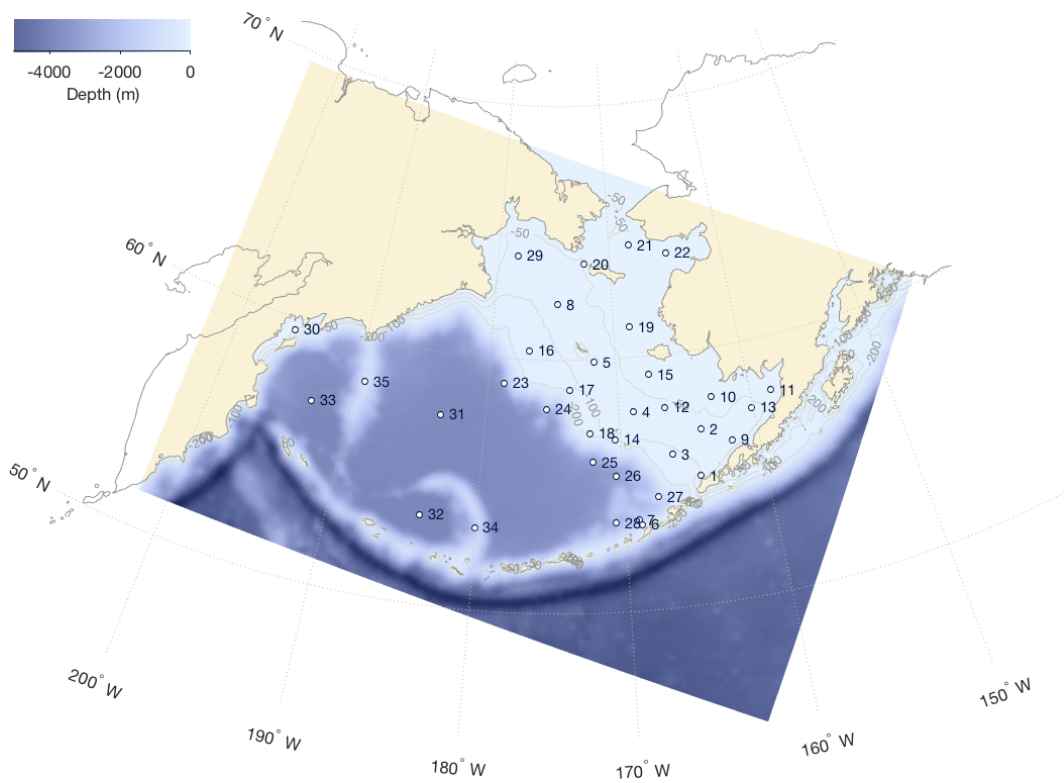


**Figure 9** – The Bering 10K ROMS domain. Numbered points indicate the location of the data shown in the following figures; these locations were chosen to either correspond to observation-data collection locations (primarily moorings) or to be representative of various regions of biophysical or socioeconomic importance.

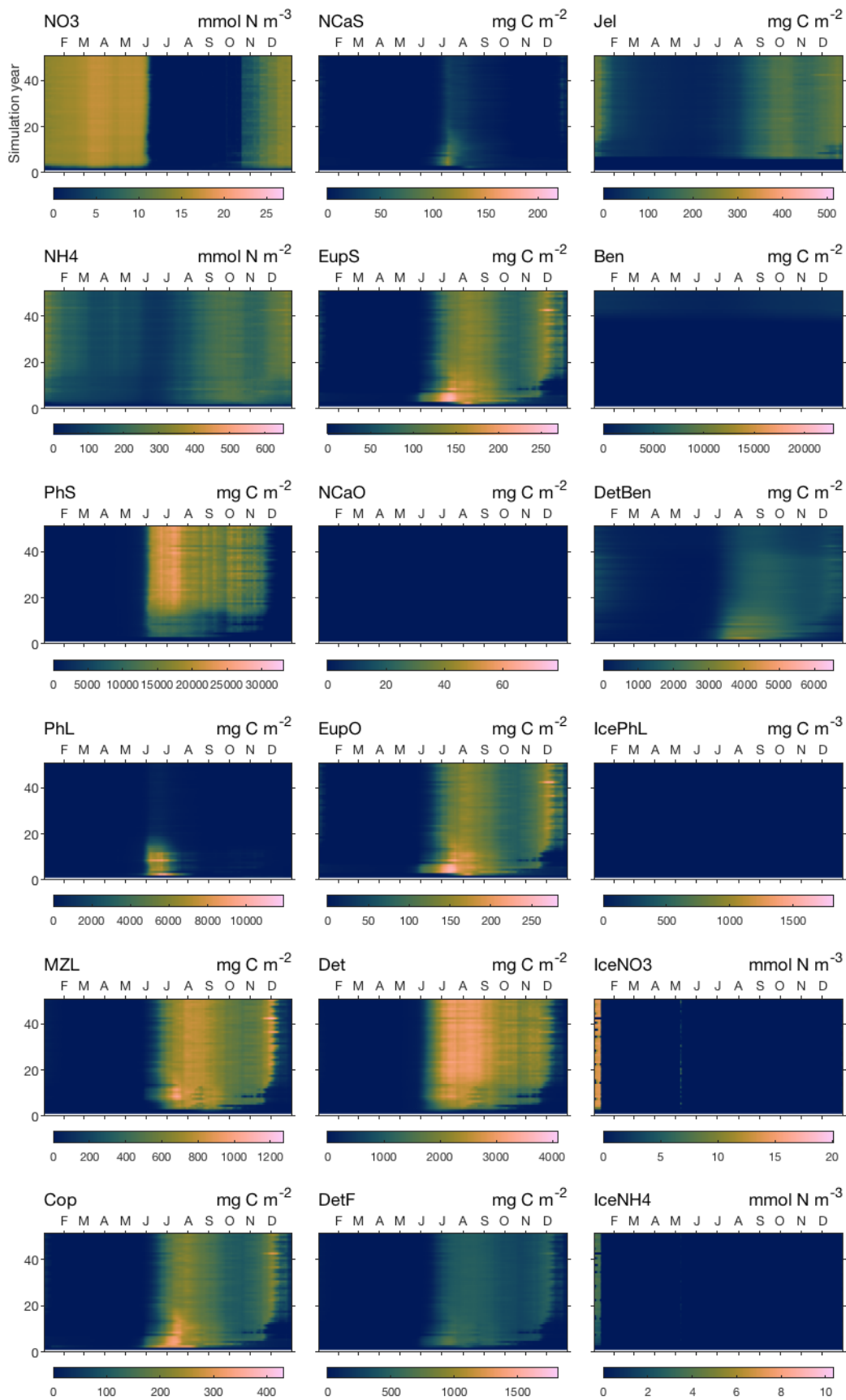


**Figure 10** – Biological prognostic variable values at Station 2 (South middle shelf), with seasonal variation along the abscissa and interannual variability along the ordinate. Nitrate values show surface concentration; ice variables indicate the concentration in the skeletal ice layer. All other variables show depth-integrated biomass.

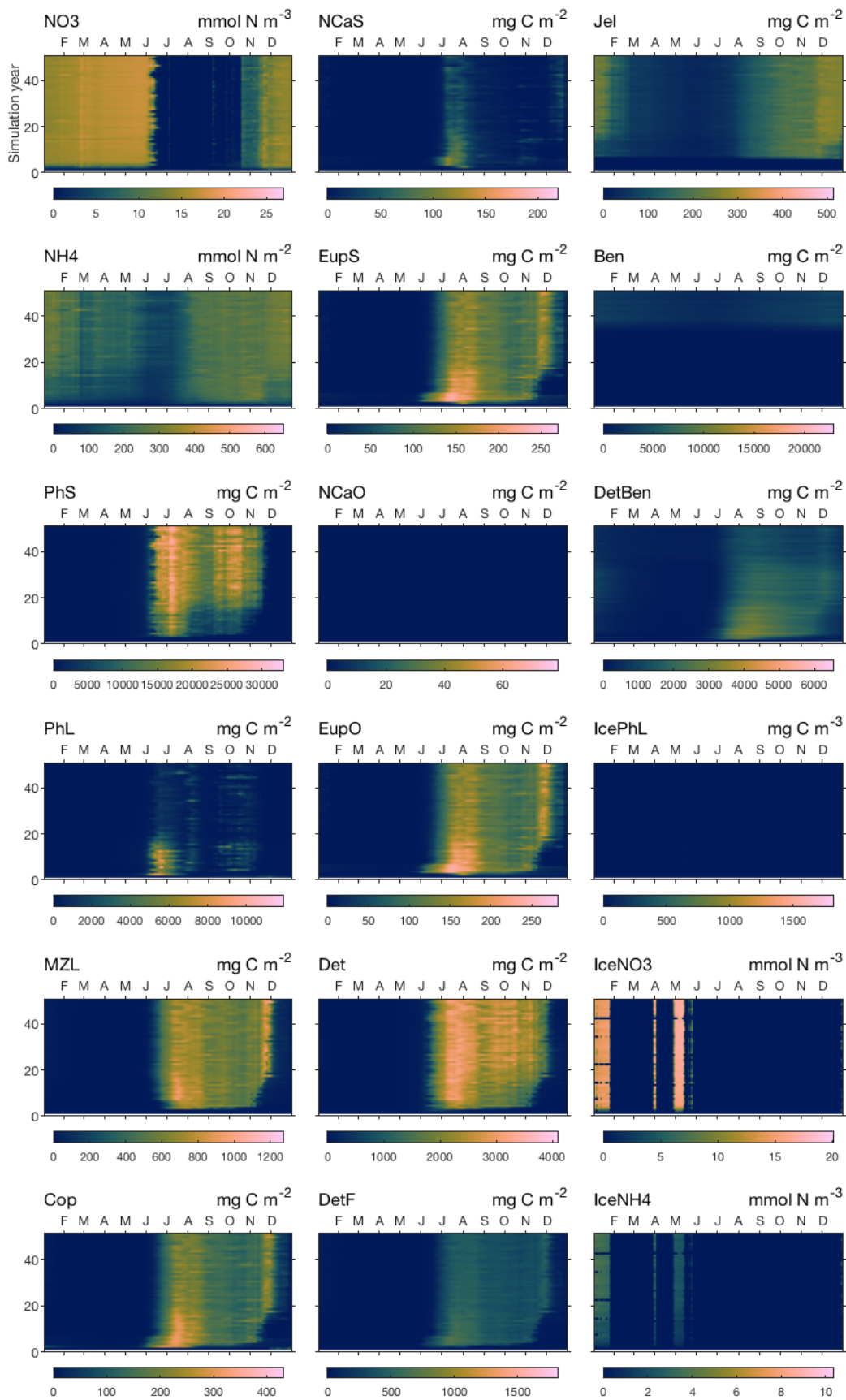


**Figure 11** – Biological prognostic variable values at Station 4 (Central middle shelf), with seasonal variation along the abscissa and interannual variability along the ordinate. Nitrate values show surface concentration; ice variables indicate the concentration in the skeletal ice layer. All other variables show depth-integrated biomass.

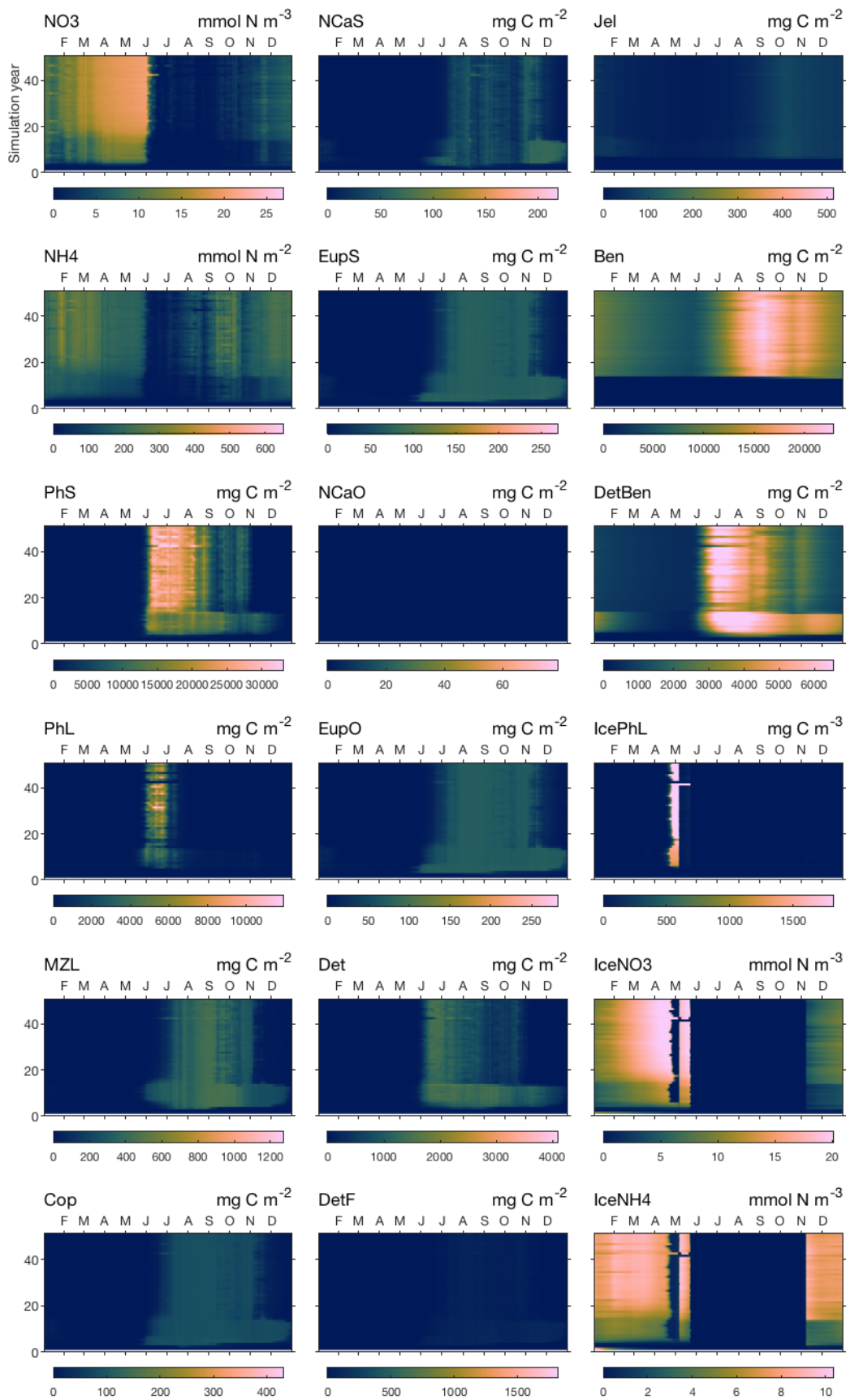


**Figure 12** – Biological prognostic variable values at Station 22 (Norton Sound), with seasonal variation along the abscissa and interannual variability along the ordinate. Nitrate values show surface concentration; ice variables indicate the concentration in the skeletal ice layer. All other variables show depth-integrated biomass.

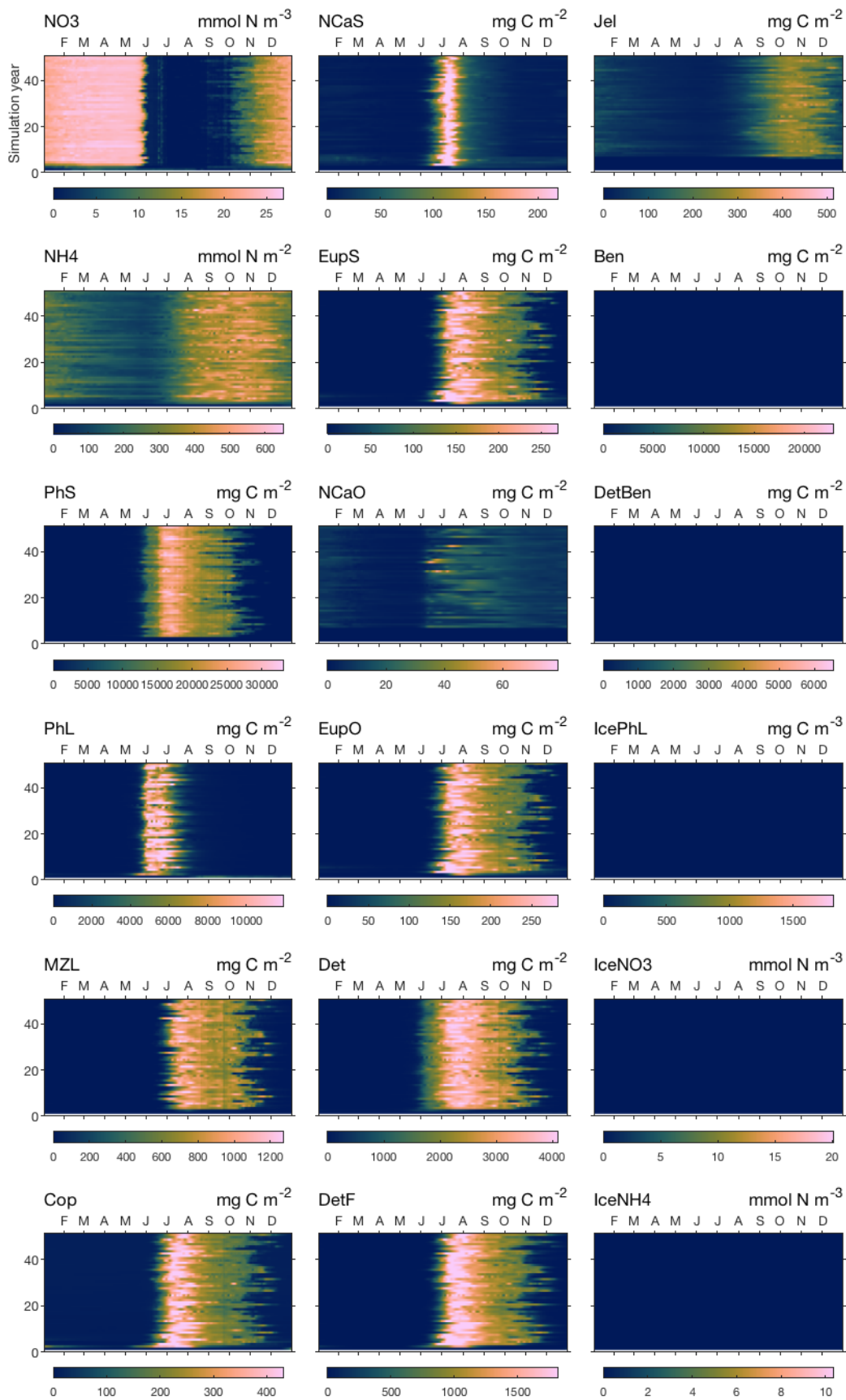


**Figure 13** – Biological prognostic variable values at Station 31 (Aleutian Basin), with seasonal variation along the abscissa and interannual variability along the ordinate. Nitrate values show surface concentration; ice variables indicate the concentration in the skeletal ice layer. All other variables show depth-integrated biomass.

## 6 References

- Arhonditsis GB, Brett MT (2005) Eutrophication model for Lake Washington (USA): Part I. Model description and sensitivity analysis. *Ecological Modelling* 187(2-3):140–178
- Arrigo KR, Sullivan CW (1992) The influence of salinity and temperature covariation on the photophysiological characteristics of Antarctic sea ice microalgae. *Journal of Phycology* 28(6):746–756
- Arrigo KR, Kremer JN, Sullivan CW (1993) A simulated Antarctic fast ice ecosystem. *Journal of Geophysical Research* 98(C4):6929–6946
- Carton JA, Giese BS (2008) A Reanalysis of Ocean Climate Using Simple Ocean Data Assimilation (SODA). *Monthly Weather Review* 136(8):2999–3017
- Coyle KO, Cheng W, Hinckley SL, Lessard EJ, Whitledge T, Hermann AJ, Hedstrom K (2012) Model and field observations of effects of circulation on the timing and magnitude of nitrate utilization and production on the northern Gulf of Alaska shelf. *Progress in Oceanography* 103:16–41
- Danielson S, Curchitser E, Hedstrom K, Weingartner T, Stabeno P (2011) On ocean and sea ice modes of variability in the Bering Sea. *Journal of Geophysical Research: Oceans* 116(June):1–24
- Denman KL, Pena MA (1999) A coupled 1-D biological/physical model of the northeast subarctic Pacific Ocean with iron limitation. *Deep Sea Research Part II: Topical Studies in Oceanography* 46(11-12):2877–2908
- Ebenhöh W, Kohlmeier C, Radford PJ (1995) The benthic biological submodel in the European regional seas ecosystem model. *Netherlands Journal of Sea Research* 33(3-4):423–452
- Frost BW (1987) Grazing control of phytoplankton stock in the open subarctic Pacific Ocean: a model assessing the role of mesozooplankton, particularly the large calanoid copepods *Neocalanus* spp. *Marine Ecology Progress Series* 39:49–68
- Gibson GA, Spitz YH (2011) Impacts of biological parameterization, initial conditions, and environmental forcing on parameter sensitivity and uncertainty in a marine ecosystem model for the Bering Sea. *Journal of Marine Systems* 88(2):214–231
- Haidvogel DB, Arango H, Budgell WP, Cornuelle BD, Curchitser E, Di Lorenzo E, Fennel K, Geyer WR, Hermann AJ, Lanerolle L, Levin J, McWilliams JC, Miller AJ, Moore AM, Powell TM, Shchepetkin AF, Sherwood CR, Signell RP, Warner JC, Wilkin J (2008) Ocean forecasting in terrain-following coordinates: Formulation and skill assessment of the Regional Ocean Modeling System. *Journal of Computational Physics* 227(7):3595–3624
- Hermann AJ, Gibson GA, Bond NA, Curchitser EN, Hedstrom K, Cheng W, Wang M, Stabeno PJ, Eisner L, Cieciel KD (2013) A multivariate analysis of observed and modeled biophysical variability on the Bering Sea shelf: Multidecadal hindcasts (1970-2009) and forecasts (2010-2040). *Deep-Sea Research Part II: Topical Studies in Oceanography* 94(2011):121–139
- Hinckley S, Coyle KO, Gibson G, Hermann AJ, Dobbins EL (2009) A biophysical NPZ model with iron for the Gulf of Alaska: reproducing the differences between an oceanic HNLC ecosystem and a classical northern temperate shelf ecosystem. *Deep Sea Research Part II: Topical Studies in Oceanography* 56(24):2520–2536
- Jassby AD, Platt T (1976) Mathematical formulation of the relationship between photosynthesis and light for phytoplankton. *Limnology and Oceanography* 21(4):540–547
- Jin M, Deal CJ, Wang J, Shin KH, Tanaka N, Whitledge TE, Lee SH, Gradinger RR (2006) Controls of the landfast ice-ocean ecosystem offshore Barrow, Alaska. *Annals of Glaciology* 44:63–72
- Kawamiya M, Kishi MJ, Suginoara N (2000) An ecosystem model for the North Pacific embedded in a general circulation model. Part I: Model description and characteristics of spatial distributions of biological variables. *Journal of Marine Systems* 25(2):129–157
- Marchesiello P, McWilliams JC, Shchepetkin A (2001) Open boundary conditions for long-term integration of regional oceanic models. *Ocean Modelling* 3(1-2):1–20

- Morel A (1988) Optical modeling of the upper ocean in relation to its biogenous matter content (case I waters). *Journal of Geophysical Research* 93(C9):10749
- Paulson CA, Simpson JJ (1977) Irradiance Measurements in the Upper Ocean. *Journal of Physical Oceanography* 7(6):952–956
- Ryabchenko VA, Fasham MJ, Kagan BA, Popova EE (1997) What causes short-term oscillations in ecosystem models of the ocean mixed layer? *Journal of Marine Systems* 13(1-4):33–50
- Saha S, Moorthi S, Pan HL, Wu X, Wang J, Nadiga S, Tripp P, Kistler R, Woollen J, Behringer D, Liu H, Stokes D, Grumbine R, Gayno G, Wang J, Hou YT, Chuang HY, Juang HMM, Sela J, Iredell M, Treadon R, Kleist D, Van Delst P, Keyser D, Derber J, Ek M, Meng J, Wei H, Yang R, Lord S, Van Den Dool H, Kumar A, Wang W, Long C, Chelliah M, Xue Y, Huang B, Schemm JK, Ebisuzaki W, Lin R, Xie P, Chen M, Zhou S, Higgins W, Zou CZ, Liu Q, Chen Y, Han Y, Cucurull L, Reynolds RW, Rutledge G, Goldberg M (2010) The NCEP climate forecast system reanalysis. *Bulletin of the American Meteorological Society* 91(8):1015–1057
- Shchepetkin AF, McWilliams JC (2005) The regional oceanic modeling system (ROMS): A split-explicit, free-surface, topography-following-coordinate oceanic model. *Ocean Modelling* 9(4):347–404
- Strom SL, Macri EL, Fredrickson KA (2010) Light limitation of summer primary production in the coastal Gulf of Alaska: Physiological and environmental causes. *Marine Ecology Progress Series* 402(May):45–57
- Strom SL, Fredrickson KA, Bright KJ (2016) Spring phytoplankton in the eastern coastal Gulf of Alaska: Photosynthesis and production during high and low bloom years. *Deep-Sea Research Part II: Topical Studies in Oceanography* 132:107–121
- Thimijan RW, Heins RD (1983) Photometric, radiometric, and quantum light units of measure: a review of procedures for interconversion. *HortScience* 18(December):818–822
- Uye S, Shimauchi H (2005) Population biomass, feeding, respiration and growth rates, and carbon budget of the scyphomedusa *Aurelia aurita* in the Inland Sea of Japan. *Journal of Plankton Research* 27(3):237–248
- Walsh JJ, McRoy CP (1986) Ecosystem analysis in the southeastern Bering Sea. *Continental Shelf Research* 5(1/2):259–288
- Walsh JJ, Rowe GT, Iverson RL, McRoy CP (1981) Biological export of shelf carbon is a sink of the global CO<sub>2</sub> cycle. *Nature* 291:197–201
- Warner JC, Sherwood CR, Signell RP, Harris CK, Arango HG (2008) Development of a three-dimensional, regional, coupled wave, current, and sediment-transport model. *Computers & Geosciences* 34:1284–1306
- Wroblewski JS (1977) A model of phytoplankton plume formation during variable Oregon upwelling. *Journal of Marine Research* 35